Contract No:

This document was prepared in conjunction with work accomplished under Contract No. DE-AC09-08SR22470 with the U.S. Department of Energy (DOE) Office of Environmental Management (EM).

Disclaimer:

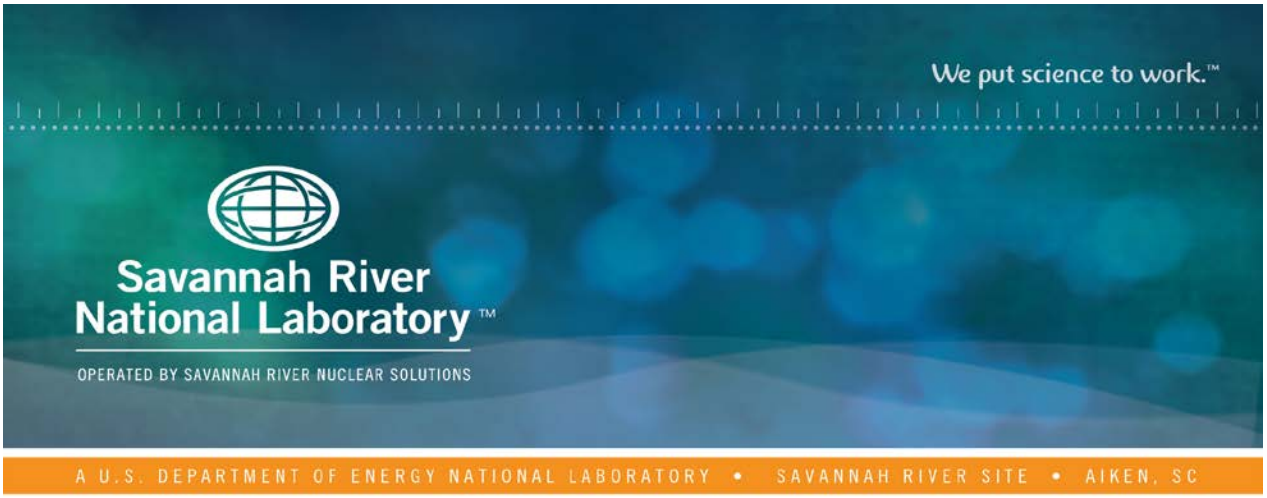

Liquid Secondary Waste: Waste Form Formulation and Qualification

A. D. Cozzi
K. L. Dixon
K. A. Hill
R. L. Nichols

July 2017
SRNL-STI-2017-00117, Revision 0

DISCLAIMER

Printed in the United States of America

Prepared for
U.S. Department of Energy

Keywords: *Hanford*
Liquid Secondary Waste
Waste Form

Retention: *Permanent*

Liquid Secondary Waste: Waste Form Formulation and Qualification

A. D. Cozzi
K. L. Dixon
K. A. Hill
R. L. Nichols

July 2017

Prepared for the U.S. Department of Energy under contract number DE-AC09-08SR22470.

Savannah River National Laboratory™
OPERATED BY SAVANNAH RIVER NUCLEAR SOLUTIONS

REVIEWS AND APPROVALS

AUTHORS:

_____

A. D. Cozzi, Wasteform Processing Technology Date

_____

K. L. Dixon, Geosciences Date

_____

K. A. Hill, Immobilization Technology Date

_____

R. L. Nichols, Geosciences Date

TECHNICAL REVIEW:

_____

D. L. McClane, Immobilization Technology, Reviewed per E7 2.60 Date

APPROVAL:

_____

C. C. Herman, Manager Date
Wasteform Processing Technology

_____

D. J. Swanberg, Manager Date
Washington River Protection Solutions

EXECUTIVE SUMMARY

The Hanford Site Effluent Treatment Facility (ETF) currently treats aqueous waste streams generated during site cleanup activities. When the Hanford Tank Waste Treatment and Immobilization Plant (WTP) begins operations, including Direct Feed Low Activity Waste (DFLAW) vitrification, a liquid secondary waste (LSW) stream from the WTP will need to be treated. The volume of effluent for treatment at the ETF will increase significantly. The powdered salt waste form produced by the ETF will be replaced by a stabilized solidified waste form for disposal in Hanford's Integrated Disposal Facility (IDF).

Washington River Protection Solutions is implementing a Secondary Liquid Waste Immobilization Technology Development Plan to address the technology needs for a waste form and solidification process to treat the increased volume of waste planned for disposal at the IDF. Waste form testing to support this plan is composed of work in the near term to provide data as input to a performance assessment (PA) for Hanford's IDF.

In 2015, three Hanford Liquid Secondary Waste simulants were developed based on existing and projected waste streams. Using these waste simulants, fourteen mixes of Hanford Liquid Secondary Waste were prepared and tested varying the waste simulant, the water-to-dry materials ratio, and the dry materials blend composition.[1] In FY16, testing was performed using a simulant of the EMF process condensate blended with the caustic scrubber—from the Low Activity Waste (LAW) melter—, processed through the ETF. The initial EMF-16 simulant will be based on modeling efforts performed to determine the mass balance of the ETF for the DFLAW.[2]

The compressive strength of all of the mixes exceeded the target of 3.4 MPa (500 psi) to meet the requirements identified as potential IDF Waste Acceptance Criteria in Table 1 of the Secondary Liquid Waste Immobilization Technology Development Plan.[3] The hydraulic properties of the waste forms tested (hydraulic conductivity and water characteristic curves) were comparable to the properties measured on the Savannah River Site (SRS) Saltstone waste form.

Future testing should include efforts to first; 1) determine the rate and amount of ammonia released during each unit operation of the treatment process to determine if additional ammonia management is required, then; 2) reduce the ammonia content of the ETF concentrated brine prior to solidification, making the waste more amenable to grouting, or 3) manage the release of ammonia during production and ongoing release during storage of the waste form, or 4) develop a lower pH process/waste form thereby precluding ammonia release.

TABLE OF CONTENTS

LIST OF TABLES

LIST OF FIGURES

LIST OF ABBREVIATIONS

BFS	Blast furnace slag
DFLAW	Direct Feed Low Activity Waste
EMF	Effluent Management Facility
ERDF	Environmental Restoration Disposal Facility
ETF	Effluent Treatment Facility
FA	Fly ash
HL	Hydrated lime
IC	Ion chromatography
ICP-AES	Inductively coupled plasma-atomic emission spectroscopy
IDF	Integrated Disposal Facility
LAW	Low Activity Waste
LSW	Liquid Secondary Waste
OPC	Ordinary portland cement
PA	Performance Assessment
PNNL	Pacific Northwest National Laboratory
QAP	Quality Assurance Program
SRNL	Savannah River National Laboratory
SRS	Savannah River Site
UDS	Undissolved solids
UPV	Ultrasonic pulse velocity
W/DM	Water to dry materials ratio
WAC	Waste Acceptance Criteria
WRA	Water reducing additive
WRPS	Washington River Protection Solutions
WTP	Hanford Tank Waste Treatment and Immobilization Plant

1.0 Introduction

The Hanford Site Effluent Treatment Facility (ETF) currently treats aqueous waste streams including evaporator condensates from the 242-A Evaporator, Environmental Restoration Disposal Facility (ERDF) leachate, and relatively small volumes of laboratory wastes. The concentrated brine from the secondary treatment train within the ETF is currently fed to a thin film dryer, producing a powdered salt waste form for disposal in drums. The ETF is also expected to treat liquid secondary waste (LSW) from Hanford Tank Waste Treatment and Immobilization Plant (WTP) operations, including Direct Feed Low Activity Waste (DFLAW). A stabilized solidified waste form is needed for disposal in Hanford's Integrated Disposal Facility (IDF).

A Secondary Liquid Waste Immobilization Technology Development Plan was generated to address the technology needs in support of the design and operation of an ETF solidification unit including waste form performance, process development, process design, and process operations.[3] Since then, a decision was made to have the waste treated off-site prior to disposal in the IDF. FY15 work focused on waste form/process development. High priority activities included waste feed envelope definition and simulant development, formulation development, and waste form qualification. A plan was developed to guide the technology development needed to support the IDF Performance Assessment (PA).[4] The waste form qualification activities needed to implement this plan are composed of work to 1) demonstrate that the waste form will meet waste acceptance criteria for the IDF, 2) demonstrate the equivalency of the performance through scale-up of the solidification process with waste forms prepared with actual radioactive wastes or simulants prepared with radioactive components, and 3) provide long-term waste form performance data and information on degradation and release mechanisms to support the IDF PA.

DOE has decided to design and build an effluent management facility to significantly reduce the volume of liquid to be returned to the Tank Farms or recycled to LAW vitrification. The EMF overheads will be combined with liquid from the LAW offgas caustic scrubber to be treated at the LERF/ETF. The ETF concentrate from this stream will be immobilized and disposed of in the IDF.

Work on this scope began in FY14 with the Pacific Northwest National Laboratory (PNNL) initiating development of updated simulants based on flowsheet analyses performed by Washington River Protection Solutions (WRPS). Work in FY15 was performed by a consortium of laboratories including Savannah River National Laboratory (SRNL) and PNNL. SRNL was requested to further the development of a waste form for liquid secondary waste to treat the combined overheads of the EMF evaporator and caustic scrubber.[5] The work was described in a Task Technical and Quality Assurance Plan.[6]

2.0 Experimental Approach

Based on the results of the matrix of formulations developed to evaluate the effects of mix components on the properties of the LSW waste form in Reference 1, the test parameters and their ranges that were investigated in FY16 testing included;

- simulant representing the EMF condensate blended with the caustic scrubber waste stream,
- water-to-dry-materials blend ratio (W/DM)—0.6 and 0.75,
- dry materials blend components—hydrated lime, ordinary portland cement, blast furnace slag, and Class F fly ash,
- dry materials blend ratios—variable, and
- mineral admixture—Xypex C-500, added as a 5% substitution into the dry blend.

The fresh properties measured in this testing were gel time, set time, free liquid, grout flowability, heat of hydration, density, and rheology. The measured properties of the cured waste forms were compressive strength, porosity, hydraulic conductivity, and the water characteristic curve.

The simulant evaluated in this study is discussed in Section 3.0. The composition of the simulant was based on a mass balance calculation for processing waste through the Effluent Treatment Facility flowsheet.[2] The 0.6 and 0.75 values of the free-water-to-dry-solids mix ratio were selected based on previous work.[1]

The dry blend mix ratio and materials were varied to evaluate the effects of both the ratio and cementitious materials blend on the fresh and cured properties listed above. The Xypex C-500 mineral admixture has been previously shown to improve leach resistance.[7]

3.0 Simulant Development and Validation

A single waste stream was evaluated in this work scope, a combined EMF overheads/caustic scrubber blend, to be processed through the current ETF flowsheet. Table 3-1 shows the targeted composition of the simulant—the EMF off-gas condensate/caustic scrubber solution that would be processed through the ETF based on the flowsheet calculations in Reference 2. Table 3-1 also shows the reagents needed to make the targeted concentration. To maintain consistency with the parallel work ongoing at the PNNL,[8] bicarbonate and mercury were omitted from the simulant.

Table 3-1. Target Concentrations and Simulant Make Up for EMF/Caustic Scrubber Simulant.

Components	Units	Concentration		Component	g/L
Chloride	g/L	0.09		NaCl	0.15
Fluoride	g/L	0.07		NaF	0.16
Sodium	g/L	45.80		Na_2SO_4	123.2
Ammonium	g/L	58.10		$NaNO_3$	26.2
Nitrate	g/L	19.10		$(NH_4)_2SO_4$	212.8
Sulfate	g/L	238.00		H_2O	854.6
Total Solids	g/L	361.16			
UDS*	g/L	~1			
density	g/mL	1.2			
pH	--	5.5			

*Undissolved Solids

The simulant was prepared and analyzed for composition using inductively coupled plasma-atomic emission spectroscopy[9] (ICP-AES) and ion chromatography[10,11] (IC). Ammonia was measured using an IC cation method.[12] The density, and solids content[13, 14] (total and dissolved in supernate) were also measured for the simulant.[15] The measured density, weight percent solids, and pH data are provided in Table 3-2 alongside the target composition, reproduced from Reference 15 and the percent difference between the measured and targeted values.

Table 3-2. Comparison of Analytical Results of Waste Simulant to Targeted Composition.

Component	Target	Units	Results	% Difference
Chloride	0.09	g/L	0.08*	13%
Fluoride	0.07	g/L	0.08*	5%
Sodium	45.80	g/L	43.55	5%
Ammonium	58.10	g/L	59.1	2%
Nitrate	19.10	g/L	18.45	3%
Sulfate	238.00	g/L	239.5	1%
solids	361.16	g/L	360.6	<1%
UDS	~1	g/L	0	--
density	1.2	g/mL	1.2142	2%
pH	5.5	--	5.47	1%
% solids	30.1	--	30.0	<1%

*Reported values are below instrument calibration curve

All the reagents added to the simulant dissolved, based on visual observations and analytical data. Soluble sodium, ammonium, sulfate, and nitrate concentrations were within 5% of the values expected based on reagent additions, Table 3-2. The minor components chloride and fluoride were within 13% of the expected values. The wt % total solids concentration was near the target value (30.1%).

4.0 Liquid Secondary Waste Formulation Development

Waste form samples were made using the formulations shown in Table 4-1. These were selected to maintain consistency with mixes prepared in Reference 8. The dry blend materials were; hydrated lime (HL),[*] ordinary portland cement (OPC)[16], blast furnace slag (BFS),[17] and Class F fly ash (FA).[18] The dry blend developed for the near neutral pH, sulfate-rich waste simulant, included hydrated lime to react with the sulfate to form gypsum and ettringite, as well as raise the pH to activate the BFS.[19] The dry material blend developed for Cast Stone is designed to work with a caustic salt solution. The mineral admixture, Xypex C-500,[†] was tested as reported in Reference 7, and is included in one formulation, added as a 5 wt% admixture addition. The remaining dry blends were renormalized to maintain a constant water-to-dry blend ratio. A Type A/Type F[20] full range water reducer[‡] was used in all mixes at an addition rate of 0.6 ml/100 g dry materials.

Table 4-1. Matrix of Formulations for this Study

Test ID	W/DM	HL/OPC/BFS/FA Blend	Mineral Admixture
FY16-1	0.60	20/35/45/00	None
FY16-2	0.75	20/35/45/00	Xypex
FY16-3	0.75	20/35/45/00	None
FY16-4	0.75	20/20/60/00	None
FY16-5	0.75	00/08/45/47	None

Depending of the properties being measured, grout mixes of 500 – 2000 ml were prepared using the setup shown in Figure 4-1. The initial agitator speed was 200 rpm and admixture was added prior to any dry material additions. As the dry blend was added, the agitator speed was increased to incorporate the dry

[*] Graymont- Rivergate Terminal, Portland, OR
[†] Xypex Chemical Corporation, Xypex Admixture C-500
[‡] BASF MasterGlenium 3030

blends In the FY15 work performed at SRNL, it was determined that some formulations required less water reducer than originally planned.[1] In this task, the full dose of admixture was used to account for the additional solids created from the reaction between the hydrated lime and the ammonium sulfate. The increased concentration of sulfate over the sulfate concentration in the simulant used in the FY15 task can produce additional gypsum or ettringite[21] during incorporation of the dry materials.

$$Ca(OH)_2 + (NH_4)_2SO_4 \rightarrow 2NH_{3(g)} + CaSO_{4(s)} + 2H_2O + \Delta H \quad (1)$$

$$3CaO \cdot Al_2O_3 + 3CaSO_4 \cdot 2H_2O + 26H_2O \rightarrow 3CaO \cdot Al_2O_3 \cdot 3CaSO_4 \cdot 32H_2O \quad (2)$$

After the dry blend was thoroughly mixed with the liquid simulant to produce a homogeneous slurry, the impeller was paused to allow entrained air to escape. Mixing continued for a total of 10 minutes. At the conclusion of mixing, the fresh properties of the grout mixture were measured.

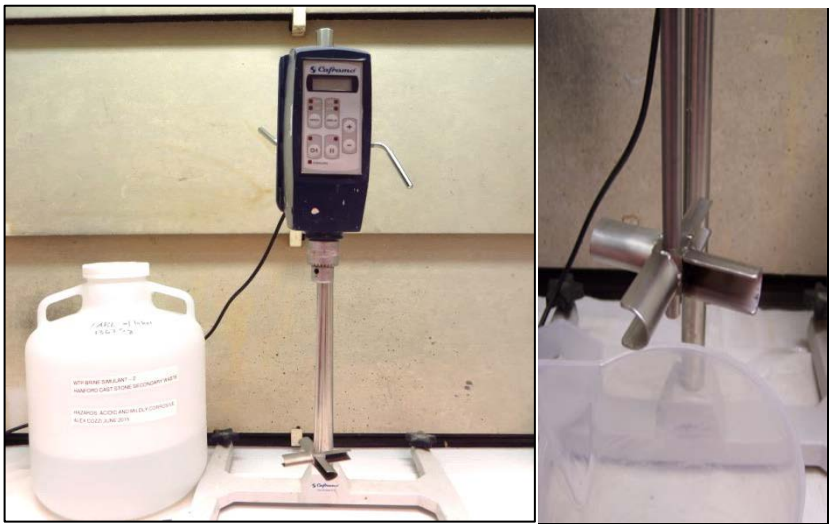

Figure 4-1. Mixer/impeller used to prepare LSW mixes.

5.0 Processing and Curing Properties

5.1 Fresh Properties

After preparation of the homogenous wet slurry mixes, properties of the freshly prepared waste form slurries were immediately measured. The properties measured and the methods used are listed in Table 5-1.

Table 5-1. Measurement Methods for Fresh Properties

Property	**Method**
Gel time	Static Cup[22]
Set time (initial, final)	Vicat[23] and Ultrasonic Pulse Velocity[24]
Free or Standing Water / Liquid	Direct Measure[22]
Grout Flowability	SRNL Modified ASTM D 6103-97[22,25]
Heat of Hydration	Isothermal Calorimetry[26]
Density	SRNL Modified ASTM D 1475-13[27]
Rheology	Flow Curve[28, 29]

5.1.1 Gel Time

Gel time is a subjective method of determining duration of grout flowability. In a continuous process, the gel time is an indication of the time after an interruption in the grout making process that is available to restart the process before it becomes necessary to perform a clean-up/shut down sequence. Gel time is also an indication of how long the placed grout (in a waste container) can maintain flowability. Gel time was measured by filling five ~100 ml containers with fresh grout. A timer was started as the first cylinder was filled. The cylinders are sequentially opened and tipped over a second container, each after an increasing amount of time. The grout is deemed gelled when the grout will no longer pour from a cylinder under its own weight. An example gel test is illustrated in Figure 5-1. In this example, the slurry successfully poured from the first three cylinders when tipped into the succeeding container. The slurry would not pour from the fourth container after resting for a period of 40 minutes after filling. Gel time is therefore approximately 40 minutes for this slurry.

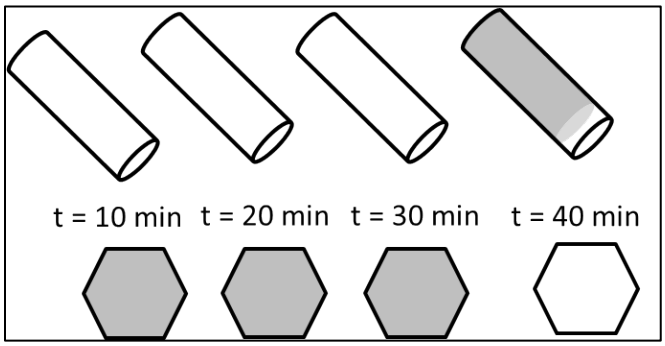

Figure 5-1. Illustration of gel time determination.

The results for the gel time tests, for each of the mixes processed, are shown in Table 5-2. Gel times measured for this set of mixes ranged from 5 minutes to greater than 2 hours. The gel time was affected by the W/DM, the blend ratio of the dry materials (FY16-3 and FY16-4), and the dry materials selection (FY16-3 and FY16-5). The effect of W/DM is demonstrated in the difference between FY16-1 and FY16-3. In these formulations, the change in a W/DM from 0.60 to 0.75 translates to a decrease from 53.9 to 48.3 wt% dry materials, resulting in an increase in gel time from 5 minutes to >20 minutes. The gel time was increased by additional water in the mix. Xypex had previously been demonstrated to extend gel time in previous testing in a simulant dry blend system,[7] however, in this testing; the waste simulant and dry blend components are different. The effect of Xypex on gel time was evaluated between formulations FY16-2 and FY16-3. Xypex contains pulverized cement and silica fume, both highly reactive components intended to decrease porosity. The reactivity of these components may contribute to the reduction in gel time measured between formulations FY16-2 and FY16-3. The reduction in gel time associated with the partial replacement of cement with slag between FY16-3 and FY16-4 may be a result of the inherent variability associated with gel time measurements. The variability between replicates was demonstrated in Reference 1. It appeared that replacing hydrated lime and some cement with fly ash in the mix increased gel time, FY16-3 and FY16-5. This observation is consistent with both the formation of gypsum and ettringite during mixing when hydrated lime is included in the dry materials blend, and the relatively slow hydration rate of Class F fly ash.

Table 5-2. Gel Times for each of the Mixes Tested.

Test ID	W/DM	HL/OPC/BFS/FA Blend	Mineral Admixture	Gel Time (min)
FY16-1	0.60	20/35/45/00	None	5
FY16-2	0.75	20/35/45/00	Xypex	5
FY16-3	0.75	20/35/45/00	None	>25
FY16-4	0.75	20/20/60/00	None	10
FY16-5	0.75	00/08/47/45	None	>120

5.1.2 *Set Time*

Set time was measured using ASTM C 191-13.[23] For this testing, the final set described in the ASTM procedure was modified to allow for up to 2 mm of penetration of the measurement needle into the grout. The modification from the ASTM is derived from the utilization of the data. The ASTM method is often used to determine when a pour can be walked on by the average worker. For waste form testing, the 2 mm set is an indication that sufficient structure was developed such that an additional lift could be placed without development of additional hydraulic head, or the waste container could be moved without disturbing its contents. The time unit for measurement is in hours, or fractions thereof. Simultaneously, the time of flight of an ultrasonic pulse (ultrasonic pulse velocity (UPV)) through a sample was measured to determine whether the sound velocity that correlates to set measured by the ASTM Vicat method is a fixed value, or is dependent on mix parameters. Set time corresponds to the development of structure from hydration and may be used as a process control point for the transport of waste packages.

The initial velocity of sound through the freshly prepared LSW mixes in this study was lower than the velocities measured for mixes in the FY15 work.[1] In contrast with the FY15 testing, the mixes in this study largely set after 24 hours rather than earlier, Table 5-3. Mix FY16-5 was not tested (Samples for compression testing did not set in the 28 day cure, Section 5.2.1). The longer set times may be attributed to the higher W/DM in these tests compared to previous testing.[1] An increase in dissolved solids in the simulant compared to previous testing may also have contributed to longer set times. As with the FY15 work, abrupt setting of these mixes made it difficult to relate the UPV response to the Vicat results. Mixes FY16-1, -2, and -3 were set at the first Vicat probe. FY16-4 was the only mix that developed structure slowly enough to track using the Vicat method. In some mixes, air gaps developed between the transducer and receiver, resulting in a sharp decrease in measured velocity. The velocity in parentheses for these mixes is the maximum velocity recorded during the test. A noticeable degradation of the polycarbonate plates that isolated the grout from the transducers was noted. The discontinuities in the UPV signal may be a result of this degradation. A review of the Cole-Parmer chemical compatibility chart notes that a 10% ammonia solution has a severe effect on polycarbonate and is not recommended for any use. Figure 5-2 shows the UPV for the mixes in this study. The plots are annotated with the Vicat results.

Table 5-3. Set time Measured by Vicat and Corresponding Sound Velocity for each Mix.

Test ID	W/DM	HL/OPC/BFS/FA Blend	Mineral Admixture	Vicat (h)	UPV (m/s)
FY16-1	0.60	20/35/45/00	None	16:24	1820
FY16-2	0.75	20/35/45/00	Xypex	44:24	1721
FY16-3	0.75	20/35/45/00	None	39:18	1473* (1784)
FY16-4	0.75	20/20/60/00	None	67:00	1428* (1865)
FY16-5	0.75	00/08/47/45	None	--	--

*Velocity when Vicat set was collected, actual velocity was higher.

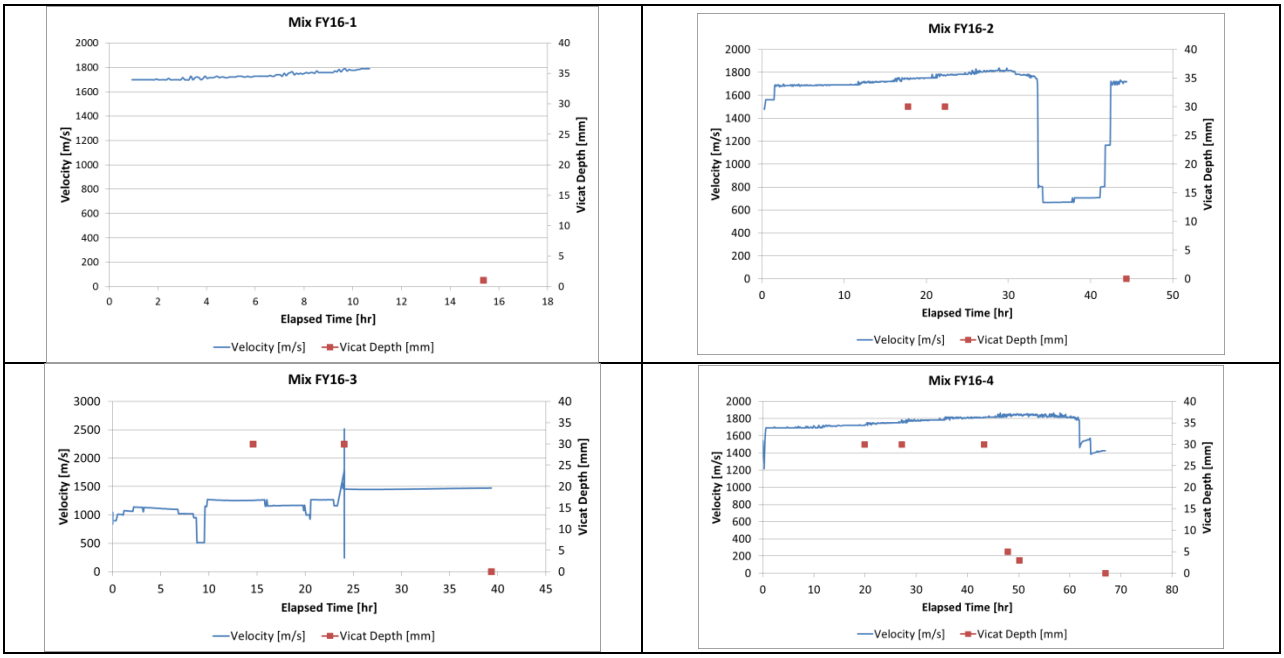

Figure 5-2. UPV response of the mixes in this study.

5.1.3 Free Liquids/Standing Water

Standing liquid was determined by measuring the residual liquid remaining after 24 hours and an additional time after that (typically 3 days ± 1 day). Duplicate samples were stored in a zip top bag with a moist towel to maintain a humid environment and to mitigate any potential moisture losses from evaporation. The volume of the residual liquid was calculated from the measured mass of the liquid recovered from the sample. The density of the liquid was assumed to be the same as the waste simulant salt solution used to prepare the grout. Although the formation of ettringite during mixing changes the composition of the pore solution, sampling of the pore solution for the porosity testing in Reference 1 revealed that the density of the extracted pore solution was similar to the starting waste simulant. The standing liquid calculation is reported as the volume of fluid collected over the volume of hardened grout calculated from the mass of the sample and the fresh density reported in Table 5-8. Standing liquid present in the sample is a preliminary indication that settling may have occurred. This may be an indication of preferential settling (segregation). Residual liquid may also be reabsorbed with time. If free liquids were present after the first measurement, a second measurement was made at a longer time to determine if the excess liquid would be reabsorbed or persist. Two of the mixes exhibited free liquid after one day, and one mix had free liquid persist to the second analysis (3 days). As can be seen in Table 5-4, free liquids were present in formulations made with reduced OPC. A second measurement was not performed on mix FY16-5 as the free liquid after one day was excessive and no further testing was warranted.

Table 5-4. Volume Percent Free Liquids Associated with Mixes.

Test ID	W/DM	HL/OPC/BFS/FA Blend	Mineral Admixture	Free Liquid (Vol %)			
				Day 1		Day 3	
FY16-4	0.75	20/20/60/00	None	2.9	2.4	0	0
FY16-5	0.75	00/08/47/45	None	15.8	14.6	nm	nm

nm- not measured

5.1.4 Grout Flowability

The grout flowability was measured by a modified ASTM D 6103-97 as described in Reference 22. A cylinder of smaller proportions than those specified by the ASTM method was used (77 mm height × 43 mm inside diameter [ID] rather than the 150 mm × 76 mm specified in the method). This method provides an indication of the ability of the grout slurry to flow after a short period of stasis. The grout flow method differs from the gel test in that the extent of flow is measured rather than a flow/no flow condition. An open-ended cylinder was placed on a flat, level surface and filled with fresh grout. The cylinder was raised so the grout would flow into a circular patty and attain symmetry. The diameter of the resulting patty was measured in two locations and the results averaged to account for any asymmetrical spread of the patty.

The extent of flow in these grout mixes was dependent upon the W/DM, and the dry blend compositions, Table 5-5. With an increased W/DM, the average flow diameter was increased. The addition of Xypex also extended the patty diameter in FY16-2 beyond that of FY16-3. This was previously noted in Cast Stone testing.[30] The substitution of 15% BFS for OPC in mixes FY16-3 and FY16-4 showed no effect. However, the change from the liquid secondary waste dry material blend to the dry blend developed for Cast Stone, FY16-5, resulted in an increase in the patty diameter of >60%. This difference in flow can be attributed to the difference in the interactions of the dry materials with the waste simulants.

Table 5-5. Average Flow Diameters of Mixes.

Test ID	W/DM	HL/OPC/BFS/FA Blend	Mineral Admixture	Flow (Patty) Diameter (mm)
FY16-1	0.60	20/35/45/00	None	115.8
FY16-2	0.75	20/35/45/00	Xypex	196.2
FY16-3	0.75	20/35/45/00	None	173.5
FY16-4	0.75	20/20/60/00	None	169.9
FY16-5	0.75	00/08/47/45	None	281.9

5.1.5 Heat of Hydration

The heat of hydration was measured by isothermal calorimetry at 25 °C in an eight-channel isothermal calorimeter.[26] Samples were prepared using the formulations in Table 4-1. The simulant waste solution was placed in a vial and the requisite amount of the pre-blended dry materials was added. The total material mixed was 18.0 grams using the same ratio of materials to prepare the mixes in Table 4-1. The vial containing the grout components was inserted into a Resodyne acoustic mixer* and mixed using a force of ~20-30 g for approximately one minute. The temperature rise during mixing, noted in Reference 1 indicated that reactions associated with the addition of hydrated lime—rise in pH, and formation of gypsum and ettringite—generate a significant amount of heat during the mixing process. Mixing for a minute in the acoustic mixer may facilitate measurement of the heat generated early in the mixing. The acoustically mixed samples were then loaded into the isothermal calorimeter and the test initiated. Hydration in cement-based systems continues almost indefinitely. In these tests, the data was collected for at least fourteen days. The total heat evolved and power produced were normalized to the amount of dry blend materials in the sample. The acoustic mixing method does not use mechanical methods to provide shear for mixing and incorporating dry blend materials. Therefore, samples for heat of hydration were prepared without the WRA and were considered adequately mixed. Mix FY16-1 was also tested with the WRA to evaluate the effects of the WRA on the heat of reaction.

* LabRAM, Resodyne™ Acoustic Mixers, Inc., Butte, MT

The heat-of-hydration results include the total heat generated over 300 hours of testing, the maximum heat flow, and the elapsed time to reach the maximum heat flow, Table 5-6. The early generation of heat in the plots is substantiated by the "Time to Peak" column in Table 5-6, where all of the mixes peaked within 2 minutes of initiating the test. Unfortunately, this peak is convoluted with the "return to baseline" signal of the instrument and cannot be isolated. The mixes containing hydrated lime and 35% OPC all produced a second peak within 24 hours. When 15% of the OPC was substituted with BFS, the second peak was delayed to 50 hours and diminished in magnitude. The double peaks are not present in the mix prepared without hydrated lime that, after the initial peak, did not exhibit any changes in slope. Although formulated by the manufacturer as a set accelerator, in these formulations the WRA also performs as a set retarder, delaying and dampening the heat generation peak. The total heat generated from cement and water is greater than 450 J/g. The generated heat captured in this task are similar to each other, with the exception of FY16-5, but somewhat lower than the typical cement/water value. For the formulations containing hydrated lime, this shortfall can be attributed to the heat generated during mixing. That is, heat generated from the reactions that precipitate gypsum and form ettringite during mixing, precede the collection of heat generation data in the calorimeter. The mix that did not contain hydrated lime and had 8% OPC did not generate appreciable heat and reached 54 J/g after 400 hours.

Table 5-6. Total Heat, Heat Flow, and Time to Maximum Heat Flow for Mixes at 25 °C.

Test ID	W/DM	HL/OPC/BFS/FA Blend	Mineral Admixture	Heat @ 300 hr (J/g)	Time to Peak (hh:mm)		Heat Flow at Peak (mW/g)	
					1st	2nd	1st	2nd
FY16-1	0.60	20/35/45/00	None	267	00:02	09:50	39.1	0.86
FY16-1[a]	0.60	20/35/45/00	None	260	00:02	16:55	39.3	0.72
FY16-2	0.75	20/35/45/00	Xypex	273	00:02	15:25	35.9	0.69
FY16-3	0.75	20/35/45/00	None	281	00:02	14:12	45.4	0.70
FY16-4	0.75	20/20/60/00	None	232	00:02	50:11	37.7	0.44
FY16-5	0.75	00/08/45/47	None	50.2	00:02	--	28.3	--

[a] Prepared with WRA

5.1.6 Density

The density of freshly prepared grout waste form slurries was measured using a cup of known volume as described in Reference 27, with the exception that the cup volume is checked, but not calibrated per the procedure. Prior to testing, the volume of the sample cup was verified with deionized water at room temperature. After the initial volume check, only the tare weight of the cup was recorded assuming that the volume of the stainless steel cup remained constant throughout the testing period. To measure the fresh density, the sample cup was filled with fresh slurry to form a meniscus. The container was capped and the excess material expressed from the overflow was wiped away. The sample cup was wiped to remove any material from the outer surfaces and then was placed on a balance to obtain the mass of the sample. The fresh density is calculated from the mass of the sample divided by the known volume of the sample cup.

The cured density of each monolith was measured geometrically on the 28-day compression cylinders prior to testing. The diameter of each cylinder was measured near the top, middle, and bottom. The length or each cylinder was then measured three times, rotating the cylinder ~ 120° between measurements. The average value of the diameter measurements and the average value of the overall length measurements were used to determine the volume of the monolith. Each monolith was weighed to determine its mass. The mass of the monolith was divided by the determined volume to calculate the cured density.

In addition, the grout density for each formulation was calculated using the rule of mixtures. The density of the waste simulant was taken from Table 3-2. The density of each of the dry material blends was calculated from the densities of the individual components, Table 5-7. The densities of each of the dry materials were measured using a helium pycnometer.*

Table 5-7. Density of the Individual Dry Materials.

Component	Density (g/cm^3)
Blast furnace slag	2.88
Class F fly ash	2.59
Ordinary portland cement	3.20
Hydrated lime	2.21
Xypex C-500	2.80

The density of each formulation determined by the three methods described above is shown in Table 5-8. The results indicate fairly good agreement among the methods to determine density for each mix. The results indicate that the fresh density can have variability introduced by the air entrained during mixing that reduces the density. Therefore, the density can be affected by the rheological properties of the fresh mix—mixes with higher yield strength and plastic viscosity can entrain air and increase the variability of the density measurement. In these tests, where gypsum and ettringite are formed from the reaction between the waste simulant and the dry materials, the calculated density may not be as accurate as those calculated for the LAW grout waste forms. It is apparent from the data that the density of these mixes is primarily dependent on the W/DM, exhibiting higher densities for lower W/DM due to the large difference between simulant density (1.2 g/ml) and the density of dry blend components (2.2-3.2 g/ml). Mixes formulated with a higher density simulant may exhibit larger density variations based on dry blend composition (i.e. lime/cement substitutions could exhibit a large difference).

Table 5-8. Density of the Mixes Measured Fresh, Cured, and Calculated.

Test ID	W/DM	HL/OPC/BFS/FA Blend	Mineral Admixture	Fresh (g/cm^3)	Cured (g/cm^3)	Calculated (g/cm^3)
FY16-1	0.60	20/35/45/00	None	1.74	1.74	1.76
FY16-2	0.75	20/35/45/00	Xypex	1.64	1.64	1.69
FY16-3	0.75	20/35/45/00	None	1.69	1.64	1.69
FY16-4	0.75	20/20/60/00	None	1.68	1.61	1.68
FY16-5	0.75	00/08/45/47	None	1.69	--	1.67

5.1.7 Rheology

The flow curve used to measure the yield stress and plastic viscosity of the grout slurry mixture is a linear ramp for five minutes to 300 s^{-1}; a 30 second hold; and a linear ramp for five minutes to 0 s^{-1}. It is assumed that during the flow curve measurements in this task, time dependent issues that could be associated with the grout slurries (e.g. chemical reactions) do not affect the measurement. The most common rheological model used to describe the flow of concrete, mortars, and cement is the Bingham Plastic model.[31,32] The rheological properties of the fresh grout waste form slurry were measured using a bob and cup method described in Reference 29.

* Micromeritics AccuPyc II 1340, Norcross, GA

All the flow curves were obtained with a rotoviscometer*, using the MV2 cylindrical rotor and cup configuration. The MV2 bob was selected given its range of measurement and design (e.g., the only shearing surface is the cylinder itself). The rheological measurements were obtained at the temperature of the slurry (i.e., the temperature as measured at the end of the mixing activities). Thixotropic response was expected, given that some of the slurries start developing structure when shearing (mixing) stops. Table 5-9 shows the yield stress and plastic viscosity determined by applying the Bingham Plastic model. In this study, all the down flow curves were analyzed as Bingham Plastic fluids.

Table 5-9. Yield Stress and Plastic Viscosity Determined by Fitting Rheograms to a Bingham Plastic Model.

Test ID	W/DM	HL/OPC/BFS/FA Blend	Mineral Admixture	Plastic Viscosity (cP)	Yield Stress (Pa)	Fitted Shear Range (1/s)
FY16-1	0.60	20/35/45/00	None	237.9	83.6	30 – 300
FY16-2	0.75	20/35/45/00	Xypex	83.6	21.2	15 – 300
FY16-3	0.75	20/35/45/00	None	93.5	42.6	30 – 300
FY16-4	0.75	20/20/60/00	None	123.1	73.7	30 – 300
FY16-5	0.75	00/08/45/47	None	56.0	6.2	15 – 300

The plastic viscosities for the mixes ranged from 56.0 – 237.9 cP, a wider range than the 4.2 – 72.5 cP range in the FY15 testing. The yield stress for the mixes in this study ranged from 6.2 – 83.6 Pa, lower than the yield stress for all of the FY15 formulations, 127 – 456 Pa. The lower yield stresses can be attributed to the increase in W/DM. This is demonstrated in the difference between formulations FY16-1 and FY16-3, where the only change was the W/DM. The substitution of a portion of the OPC for BFS between formulations FY16-3 and FY16-4 led to a marked increase in both the plastic viscosity and yield strength. One possible explanation for this is the interaction of the WRA with OPC is more effective than with BFS.[33] There are also potential WRA degradation reactions with the waste simulants that may influence the effectiveness of the WRA and the subsequent rheological properties of the fresh grout.[34] Figure 5-3 shows the rheograms for the formulations tested in this study.

* Haake RS6000, ThermoFisher, Waltham, MA

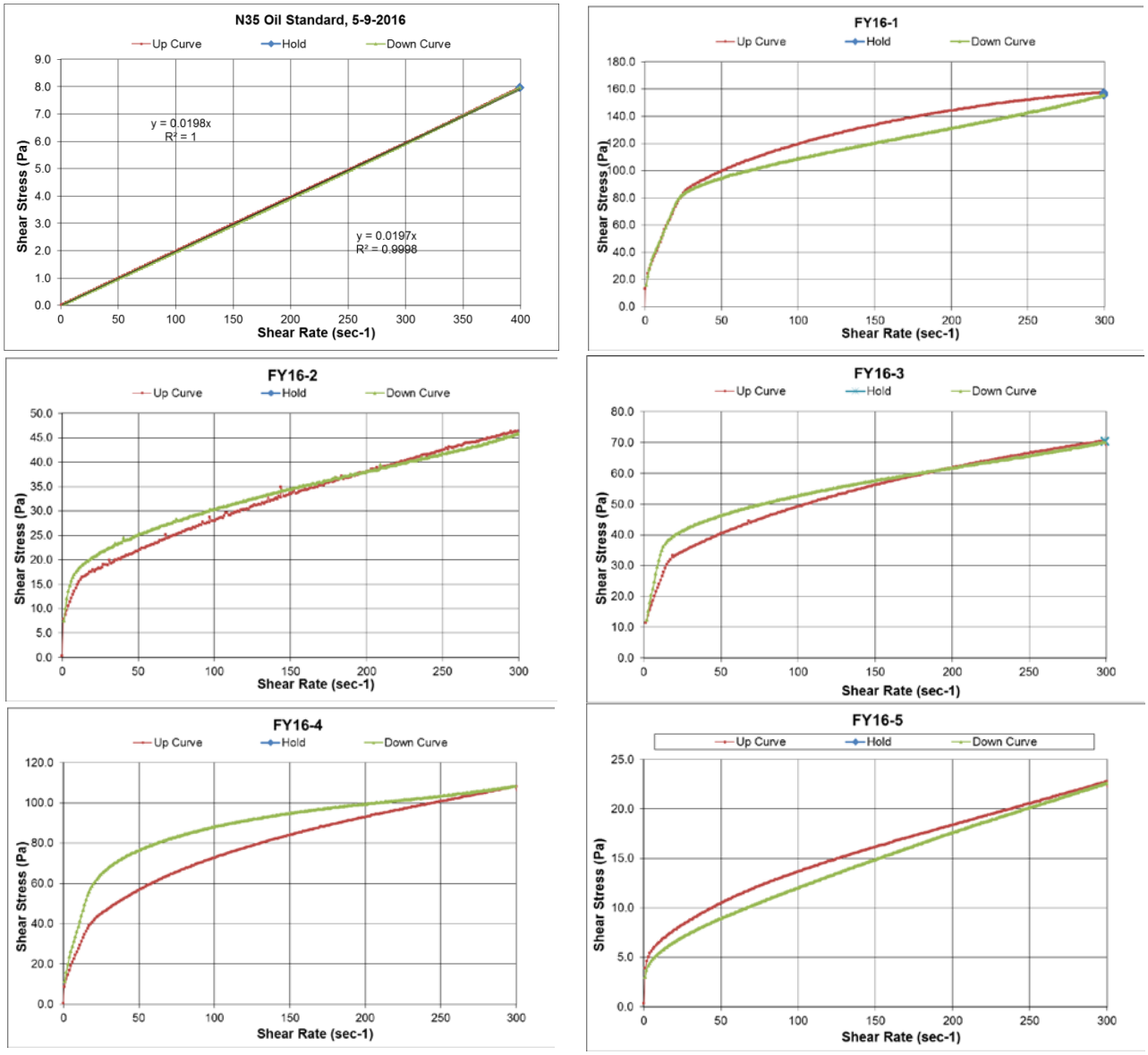

Figure 5-3. Rheograms for oil standard and formulations prepared in this study.

5.2 Cured Properties

Samples of the grout slurries that were cast into 2 in x 4 in molds, stored in a zip top bag with a moist towel overnight while structure developed, then vacuum sealed until analysis. Cured samples were analyzed for properties identified in Table 5-10.

Table 5-10. Cured Properties Analytical Methods

Property	Method
Compressive Strength	Uniaxial compression ASTM C 39/39M-15a[35, 36]
Porosity	Gas Pycnometry ASTM D 5550-14 [37] and Mass Loss[38]
Hydraulic Conductivity	Permeameter ASTM D 5084-10[39]
Water Characteristic Curve	Soil Water Characteristic Curve ASTM D 6836-02[40]

5.2.1 Compressive Strength

Compressive strength is commonly used as an indication of the overall quality (mix design and preparation) of the sample. After curing for 3, 7, or 28 days, 2 in diameter x 4 in height cylindrical samples were demolded and tested for compressive strength in triplicate using unbonded caps.[35] The demolded samples were inspected for parallel surfaces. If an end of a sample showed a clear deviation from flatness, the excess material was removed. If the imperfection was a small nodule, coarse grit sandpaper was used to true the surface. For larger imperfections, the sample surface was trimmed using a miter saw. The resulting cylinder was measured as described in Section 5.1.6, capped, and tested. Compressive strength testing was conducted using a hydraulic compression tester.* The compressive load was applied until the load indicated by the equipment was reduced to 75% of the maximum load applied to the specimen. The loading rate was set at approximately 0.25 MPa/s (29.4 kN/min) as specified by Reference 35. It should be noted that a noticeable ammonia odor was emitted from samples after compression testing.

The compressive strength target is a minimum of 3.4 MPa (500 psi) to meet the requirements identified in Reference 3. Both the cure time and the W/DM affected the compressive strength, Table 5-11. Testing of mix FY16-1 at 3, 7, and 10 days provides insight into the development of strength in this family of formulations. At three days, the samples had developed sufficient structure to be tested. The three day compressive strength did not meet the desired disposal criterion of 500 psi. There was, however, no significant difference between the compressive strength measured after 7 days and 28 days. The samples prepared without hydrated lime, FY16-5, were not set sufficiently after 28 days to test. As discussed in Reference 1, the addition of hydrated lime promotes the formation of gypsum and ettringite, which both can contribute to early strength (28 days). Class F fly ash is slower to react and can take several more weeks to fully develop strength.[41]

Table 5-11. Compressive Strength of Triplicate Cylinders of each Mix.

Test ID	W/DM	HL/OPC/BFS/FA Blend	Mineral Admixture	Cure Time (days)	Compressive Strength (psi)			
					-1	-2	-3	Avg
FY16-1	0.60	20/35/45/00	None	3	442	458	484	461
FY16-1	0.60	20/35/45/00	None	7	1350	1395	1422	1389
FY16-1	0.60	20/35/45/00	None	28	1425	1324	1362	1370
FY16-2	0.75	20/35/45/00	Xypex	28	976	967	973	972
FY16-3	0.75	20/35/45/00	None	28	1181	1172	1171	1175
FY16-4	0.75	20/20/60/00	None	28	1107	1200	1253	1187
FY16-5	0.75	00/08/45/47	None	28	nm	nm	nm	--

nm – not measured

* Humboldt Manufacturing, Schiller Park, IL, model #HCM-0300 with Test Mark Industries, LXI data acquisition system

5.2.2 Porosity

The porosity was measured on samples prepared in glass vials using the method in Section 5.1.5. After mixing, sample vials were closed with crimp fittings, vacuum sealed, and left to cure for two weeks. The cure time was based on the compressive strength results in Table 5-11 showing that ultimate strength was achieved in seven days. Since there is not a baseline process in the Hanford flowsheet for preparing this waste form, sample preparation methods were chosen to reduce the influence of sample preparation on measured properties. Therefore, the potential reduction of entrained air compared to the mechanical mixing methods should be noted when evaluating results. The volume of as-made and dried samples were measured by ASTM method D 5550-14, Reference 37 using a helium pycnometer.* The samples were trimmed to a right cylinder and the volume measured. After measurement, the samples were heated at ~105 °C overnight. The mass was measured daily until the mass change on consecutive days was <5%. The volume was then measured on the dried samples. The porosity was then calculated by dividing the volume of the dried sample by the geometric volume calculated from the diameter and height of the sample. The initial saturation of the samples is not known, therefore the geometric value was used rather than the envelope volume measured by the pycnometer. In previous work, the porosity was calculated as the volume of the pore solution by assuming the mass loss was due entirely to water, and dividing by the density of the pore solution and the mass fraction of water in the pore solution.[38] In this waste form, there was sufficient reaction between the salt solution and the dry materials such that the assumption that the pore solution was similar to the initial waste simulant was not justified. As such, the density of the pore solution was assumed to be 1.08 g/cm^3, as measured for a similar waste form in Reference 1. Table 5-12 shows the moisture content (% mass loss) of each sample and the volume percent porosity for each of the mixes determined by each method. The moisture content may not be an accurate representation of the free water present, as ettringite is known to release bound water at temperatures above 80 °C.[42] The additional loss of water associated with the conversion of ettringite to meta-ettringite—which has 10-13 H_2O per mole as opposed to 30-32 H_2O in ettringite—may result in reporting of a larger porosity than actually present.

FY16-1—the sample with the lowest W/DM—had the lowest porosity. This porosity is significantly lower than similar samples prepared in Reference 1, ~45-46% as compared to 58-59%. FY16-1 was made using the same W/DM and dry material blend as samples 6 and 8 in Reference 1. The simulants were chemically similar but varied in density and solids content. The current simulant had a density of 1.22 g/cm^3 and 30 wt% solids, Table 3-2, whereas the simulant in Reference 1 had a density of 1.13 g/cm^3 and 18 wt% solids. As expected, the porosities of the mixes prepared at a W/DM of 0.75 were higher than the mix at a W/DM of 0.60. The porosity calculated from volume measurements were consistent with the porosity values calculated from mass loss during drying.

Table 5-12. Porosity Calculated using Method from References 37 and 22.

Test ID	W/DM	HL/OPC/BFS/FA Blend	Mineral Admixture	Moisture Content (Mass %)	Porosity[a] (vol %)	Porosity[b] (vol %)	Porosity[c] (vol %)
FY16-1	0.60	20/35/45/00	None	28.6	44.9	46.1	41.5%
FY16-2	0.75	20/35/45/00	Xypex	35.3	54.7	53.6	48.2%
FY16-3	0.75	20/35/45/00	None	34.7	53.6	52.8	47.5%
FY16-4	0.75	20/20/60/00	None	36.6	56.4	54.5	49.1%

[a]Calculated from volume change measured using helium pycnometry.
[b]Calculated from mass loss using pore solution density from FY15 testing.

* Micromeritics AccuPyc II 1340, Norcross, GA

[c]Calculated from mass loss using simulant density from FY16 testing.

5.2.3 Hydraulic Conductivity

Hydraulic conductivity (K) is the coefficient used to express the ease with which a fluid passes through a porous matrix. K therefore depends both on degree of saturation as well as matrix and fluid properties. The relevant fluid properties are density and viscosity. The relevant properties of the solid matrix are water saturation and factors effecting pore geometry such as grain size distribution, grain shape, tortuosity, porosity etc. Numerical models of fluid flow in porous matrices such as Saltstone and Cast Stone typically use saturated K (Ksat), and a correlation between K and saturation determine the K for calculations of fluid flow and contaminant transport. These models have been successfully used to simulate fluid flow and contaminant transport through porous waste forms and can be used to model the transport of water through the LSW waste form.

Four samples from the screening test matrix, shown in Table 4-1, were analyzed to determine the saturated hydraulic conductivity. Mix FY16-5 was not tested as other properties eliminated it from consideration. As with the samples for compressive strength, 2 x 4 inch cylindrical samples were demolded. The samples were trimmed to have parallel faces and a height of approximately 2 inches—a sample aspect ratio of 1. After being trimmed, the samples were submerged in deionized water and placed under vacuum to displace air and saturate the samples. Any leaching related to saturation and testing with deionized water would return a higher hydraulic conductivity (conservative). Following vacuum saturation, the samples were tested in a flexible wall permeameter using Method C in Reference 39 for determining hydraulic conductivity of saturated materials. The samples were loaded into a tri-axial cell with a glass fiber filter, porous stainless steel disk and cap on both ends with a surrounding rubber membrane held in place with O-rings. Once the samples were placed in the permeameter, saturation was completed on the samples using back pressure to remove any residual gas bubbles. The permeation was started by increasing the influent pressure while keeping the effluent pressure constant to maintain the back-pressure. Testing was deemed complete when at least four values of steady hydraulic conductivity were obtained each work day.

To mitigate the potential effect on the hydraulic conductivity by the osmotic pressure of the pore solution, the permeant is chosen to match the osmotic pressure of the pore solution, typically a simplified version of the waste simulant. In Reference 1, the reaction during mixing of the waste simulant and the dry blend materials was shown to change the composition of the pore solution, thus the composition of the pore simulant. Therefore deionized water was used as the permeant with the knowledge that there may be osmotic pressure effects.

The test involves measurement of the inflow and outflow of permeant. For low permeability samples the flow can be as low as tenths of a mL per day. The method allows the ratio of inflow and outflow to vary between 0.75 and 1.25. Cumulative inflow exceeded outflow in three of the 4 samples, but only mix FY16-1 had an inflow:outflow that exceeded conditions allowed by the test method. Excess inflow may have been consumed by additional hydration or other reactions that ultimately lead to a reduction in K. This is consistent with the results in Reference 1, where mixes with the same W/DM and dry blend also appeared to consume permeant.

The first measured K and last K values are reported in Table 5-13. Following the determination of the initial K, testing was continued to investigate if any temporal trends in K existed. Figure 5-4 shows the temporal variability of hydraulic conductivity with curing time (days since samples were mixed and cast into monoliths). All four of the samples had a trend of decreasing K with curing time. The hydraulic conductivities of the FY16 samples were similar to those of the samples measured in Reference 1.

Table 5-13. Initial and Final Hydraulic Conductivities Measured on Select Sample from the Test Matrix in Table 4-1.

Test ID	W/DM	HL/OPC/BFS/FA Blend	Mineral Admixture	Permeant		Test Time (d)	Hydraulic Conductivity	
				V_{in} (ml)	V_{out} (ml)		Initial (cm/s)	Final (cm/s)
FY16-1	0.60	20/35/45/00	None	2.9	2	8	$6.9x10^{-9}$	$4.4x10^{-9}$
FY16-2	0.75	20/35/45/00	Xypex	9.7	8.9	8	$3.7x10^{-8}$	$1.6X10^{-8}$
FY16-3	0.75	20/35/45/00	None	7.9	7.2	9	$3.3x10^{-8}$	$1.4x10^{-8}$
FY16-4	0.75	20/20/60/00	None	3.9	4.4	20	$2.4x10^{-9}$	$1.2x10^{-9}$

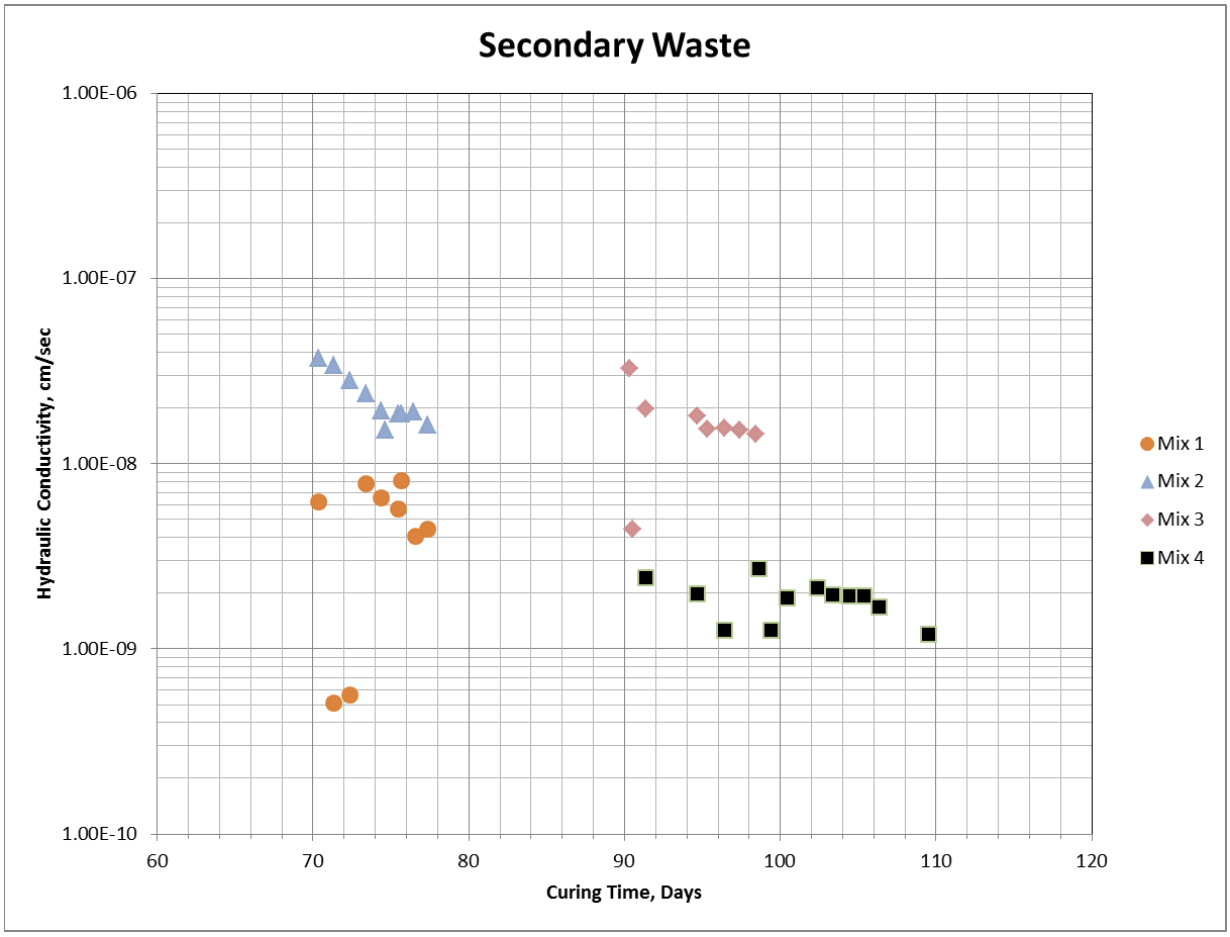

Figure 5-4. Hydraulic conductivity as a function of time for the mixes tested.

5.2.4 Water Characteristic Curve

The water characteristic curve, describes the desorption potential of a sample. When the curve is generated by the methods from Reference 40, the results, saturation as a function of suction, are presented as matric suction. Dependent upon the conceptual model selected to calculate the transport of contaminants in the IDF, these matric suction results may be used to model transport in unsaturated flow conditions.

The moisture retention properties of the four mixes, FY16-1 through -4, were analyzed to determine the van Genuchten parameters commonly used in unsaturated flow models.[43] Physical properties of the formulations are provided in Table 5-14. Physical properties were measured on samples from the controlled vapor pressure tests. Porosities reported in Table 5-14 are higher than those reported in Table 5-12 and are similar to values reported in Reference 1. Porosities reported in Table 5-14 were determined by mass loss in oven dried samples. As noted in Section 5.2.2, changes in mineral composition may affect porosities measured using mass loss. It is also worth noting that samples used in Table 5-12 were prepared and cured differently than those in Table 5-14. This may also contribute to the observed differences in porosity.

Cured samples were tested for moisture retention using three techniques; a centrifuge, measured vapor pressure (measured vapor equilibrium, chilled mirror hygrometer), and controlled vapor pressure (vapor equilibrium) methods. Based on the results in Reference 1, moisture retention measurements using the pressure plate apparatus were not attempted.

Table 5-14. Physical Properties of FY16 Formulations.

Test ID	Dry Bulk Density (g/cm^3)	Porosity (cm^3/cm^3)	Particle Density[a] (g/cm^3)
FY16-1	1.02	0.598	2.54
FY16-2	0.97	0.607	2.46
FY16-3	0.97	0.615	2.52
FY16-4	1.01	0.601	2.53

[a] Particle density calculated as $\rho_s = \rho_b/(1-\eta)$ where ρ_b is dry bulk density and η is porosity.

Testing of samples using the centrifuge generally followed Reference 40, Method E. Samples for centrifuge testing were poured in 1-inch diameter stainless steel molds and cured for a minimum of 28 days. After curing, the samples were tested in the centrifuge at increasing pressures ranging from 0.1 bar to 12 bar. No significant drainage was observed from any of the formulations over the applied pressure range.

Measured vapor pressure method testing was performed using a chilled mirror hygrometer, Reference 40, Method D. The chilled mirror hygrometer* uses the chilled mirror dew point technique to measure the total moisture potential of porous materials.[44,45] Total moisture potential is the sum of osmotic and matric potential—neglecting hydrostatic pressure and gravitational effects. Generally, osmotic potential is negligible and the total potential is assumed to be equal to the matric potential. However, in the case of the secondary liquid waste formulations, there is an osmotic component due to the high salinity of the simulants used—relative to groundwater. Therefore, the total potential measurements include the osmotic potential due to the salt content of the simulant and the matric potential due to capillarity and adsorptive forces binding moisture to the waste form particles. At the drier end of the moisture retention curve for this waste form, the osmotic potential may be significantly greater than the matric potential which is the opposite of what is typically assumed for most materials.

Samples from each of the formulations cured for a minimum of 28 days were prepared for testing by crushing the grout samples with a mortar and pestle. The crushed grout was sieved to produce bulk powder with a particle size of 1 mm or less. The chilled mirror measures the absorptive forces binding water to individual particles. Capillary contributions, and thus particle size, become negligible for matric

* Decagon Devices Model WP4C

potential values near the dry end.[46] The bulk powder from each formulation was oven dried at ~105 °C to eliminate volatile compounds that could potentially interfere with the controlled vapor pressure measurements. The bulk material was subsequently rewetted with deionized water for testing in the water potential meter. Samples were tested starting at, or near, saturation. After the initial moisture potential measurement, each sample was oven dried to achieve a lower moisture potential (drier condition). The samples were allowed to equilibrate (balance the air-water interface) for several hours between moisture potential measurements. Data from these measurements were used to establish a drying (desorption) moisture characteristic curve. This data is tabulated in Appendix A. At the conclusion of the drying tests, samples were sequentially rewetted with deionized water to create a wetting (adsorption) moisture characteristic curve, Appendix B.

A controlled vapor pressure method (vapor equilibrium) was used to provide a comparison to the measured vapor pressure method implemented with the water potential meter. For this method, intact wafers approximately 10 mm thick (~25 g) were placed above a saturated salt solution inside a sealed container. The saturated salt solution produces a constant relative humidity (RH) in the headspace of the sealed container.[47] Relative humidity is then related to total water potential using the Kelvin equation.[44] At equilibrium, Reference 44 assumes the material attains the same total potential as the vapor in the headspace of the container. As with the measured vapor pressure method, this method is influenced by both osmotic and matric potential.

Each wafer was weighed prior to placing it in the sealed container with the standard salt solution. Periodically, the samples were removed and weighed to determine whether equilibrium had been reached. When the mass change between successive readings was generally less than 0.1g, testing was stopped. The controlled vapor pressure tests lasted from 76 to 113 days. At the conclusion of the controlled vapor pressure testing, wafers from each formulation were used to determine dry bulk density and porosity. After measuring the diameter and thickness of each wafer, the samples were vacuum saturated in tap water. Periodic weight checks were used to determine when the samples were saturated. Once saturated, the samples were weighed and then oven dried at 90 °C. The porosity and dry bulk density of each wafer was determined using the physical measurements and the final dry mass.

The results from the dry bulk density and porosity measurements are provided in Table 5-14. The dry bulk density of the four secondary waste formulations ranged from 0.97 to 1.02 g/cm^3 and porosity ranged from 0.598 to 0.615. These measurements are based on the 24 samples used in the controlled vapor pressure experiment. Additionally, three samples from secondary waste formulation 16-1 were tested for dry bulk density and porosity as received for validation of the wafers from the controlled vapor pressure test. The average bulk density of the mix 16-1 confirmation samples was 1.13 g/cm^3 compared to 1.02 g/cm^3 from the controlled vapor pressure wafers. The average porosity of the confirmation samples was 0.562 compared to 0.598 for the controlled vapor pressure wafers. These values compare favorably and corroborate the results from the controlled vapor pressure wafers. As received saturation fraction was determined for the 22 controlled vapor pressure wafers and was found to range from 0.96 to 1.00. The results from the controlled vapor pressure tests are in Table 5-15. The results from the drying and wetting measured vapor equilibrium tests along with the results from the controlled vapor equilibrium test are plotted in Figure 5-5 through Figure 5-8.

The moisture retention data from both the drying and wetting measured vapor equilibrium tests were analyzed to estimate the parameters α, n and m in the van Genuchten functional form[43]

$$S_e = \frac{1}{[1+(\alpha\varphi)^n]^m}, \quad (3)$$

where α is related to the inverse of the air entry suction and, *n* is a measure of the pore-size distribution, and where effective saturation is defined by

$$S_e \equiv \frac{\theta-\theta_r}{\theta_s-\theta_r} = \frac{S-S_r}{1-S_r}. \quad (4)$$

The subscripts for θ, water content, refer to saturated (s) and residual (r) conditions. Using S_e the relative hydraulic conductivity K was calculated at incremental pressure heads using the Mualem-van Genuchten type function

$$K = S_e^L \left[1 - \left(1 - S_e^{1/m}\right)^m\right]^2, \quad (5)$$

where *L* is an empirical pore-connectivity parameter and is assumed to be 0.5. Good agreement is noted between the measured and controlled vapor equilibrium data for all four formulations. These data were analyzed to determine the van Genuchten curve fitting parameters using a non-linear regression analysis in Microsoft Excel.[48] The van Genuchten transport parameters for the drying and wetting datasets are presented in Table 5-16. Plots of the van Genuchten curve fit for each formulation and dataset are presented in Appendix C. Figure 5-9 shows a plot of the relative permeability function for all four secondary waste formulations testing using the combined measured vapor equilibrium dataset (drying and wetting). All four formulations exhibit similar characteristics as expected given their similarity in composition. A comparison of the relative permeability function for each secondary waste formulation as determined using measured vapor equilibrium and controlled vapor equilibrium is in Appendix D. These figures show that the relative permeability function produced by the two methods are similar but the results from the controlled vapor equilibrium data imply more drainage over the wetter end of the moisture retention curve.

Table 5-15. Moisture Retention Data Measured using Controlled Vapor Pressure Method.

Mix	RH (%)	Gravimetric Moisture Content (cm^3/cm^3)	Volumetric Moisture Content (cm^3/cm^3)	Saturation (fraction)	Total Potential (bar)	Total Potential (cm H_2O)
FY16-1	0.98	0.505	0.516	0.864	37.7	38439
	0.85	0.454	0.465	0.777	236.8	241516
	0.75	0.398	0.407	0.681	390.7	398404
	0.59	0.308	0.315	0.527	759.7	774713
	0.12	0.217	0.223	0.372	3002.7	3062027
FY16-2	0.98	0.575	0.555	0.913	37.7	38439
	0.85	0.452	0.436	0.718	236.8	241516
	0.75	0.396	0.382	0.629	390.7	398404
	0.59	0.320	0.309	0.509	759.7	774713
	0.12	0.254	0.245	0.404	3002.7	3062027
FY16-3	0.98	0.562	0.546	0.889	37.7	38439
	0.85	0.457	0.444	0.723	236.8	241516
	0.75	0.389	0.378	0.615	390.7	398404
	0.59	0.309	0.300	0.488	759.7	774713
	0.12	0.253	0.246	0.400	3002.7	3062027
FY16-4	0.98	0.532	0.536	0.892	37.7	38439
	0.85	0.463	0.467	0.777	236.8	241516
	0.75	0.392	0.395	0.657	390.7	398404
	0.59	0.328	0.330	0.550	759.7	774713
	0.12	0.221	0.222	0.370	3002.7	3062027

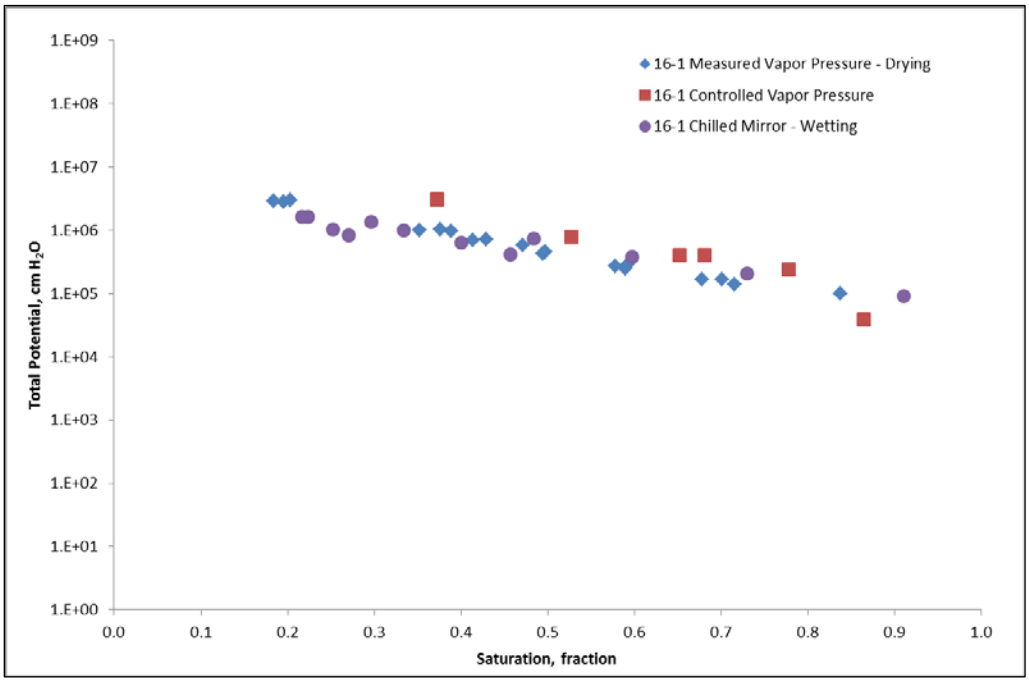

Figure 5-5. Moisture Retention Data for Secondary Waste Mix FY16-1.

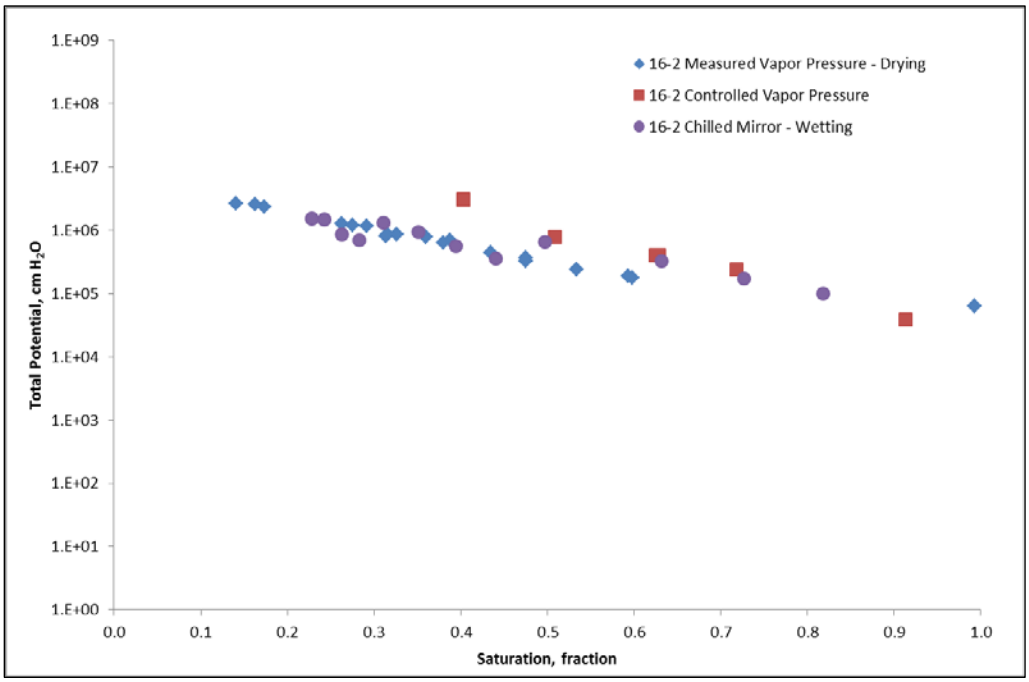

Figure 5-6. Moisture Retention Data for Secondary Waste Mix FY16-2.

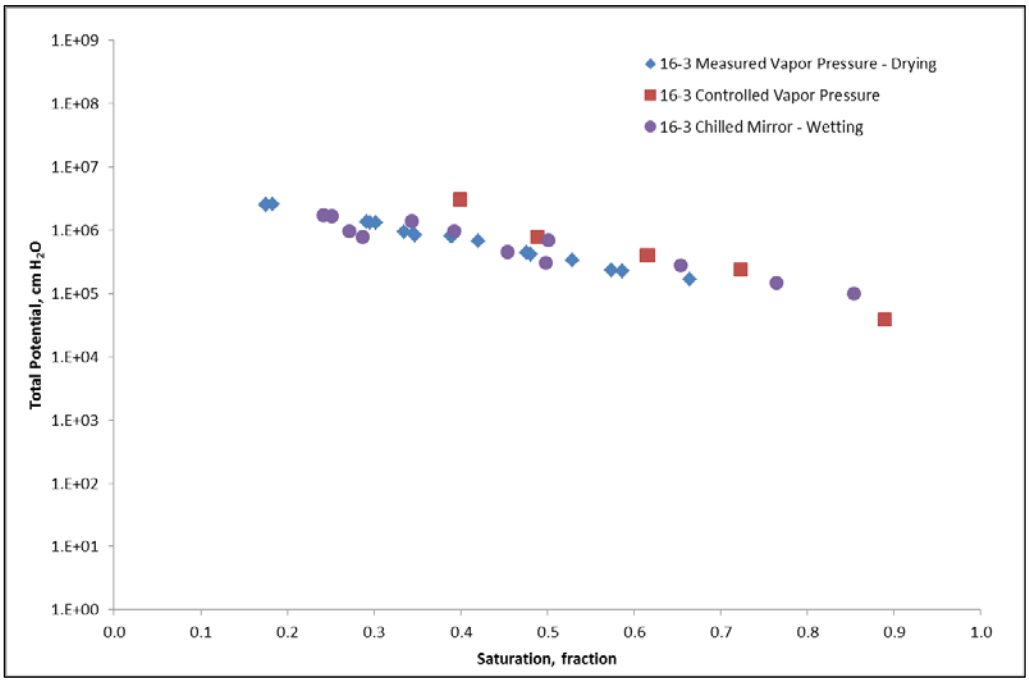

Figure 5-7. Moisture Retention Data for Secondary Waste Mix FY16-3.

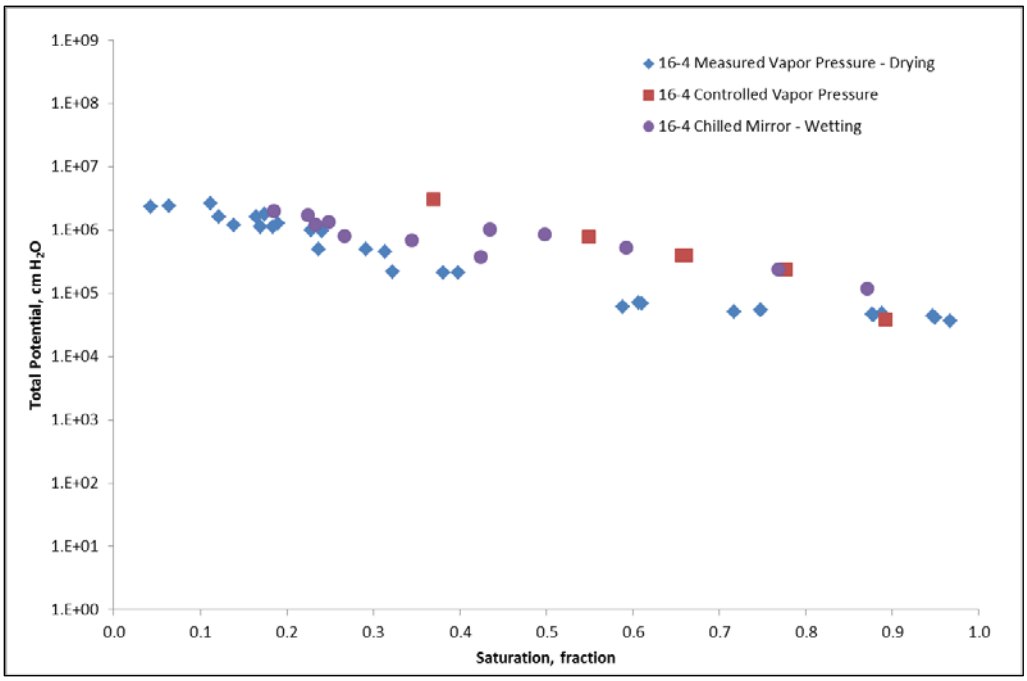

Figure 5-8. Moisture Retention Data for Secondary Waste Mix FY16-4.

Table 5-16. Van Genuchten Transport Parameters Data.

Mix[1,2]	Type	θ_s (cm^3/cm^3)	θ_r (cm^3/cm^3)	α (1/cm)	n	m	r^2
FY16-1	Measured Vapor Pressure, Drying	0.598	0.000	1.03E-05	1.44	0.31	0.98
	Measured Vapor Pressure, Wetting	0.598	0.000	7.00E-06	1.57	0.36	0.94
	Measured Vapor Pressure, Combined	0.598	0.000	6.95E-06	1.57	0.36	0.95
	Controlled Vapor Pressure	0.598	0.000	8.59E-06	1.30	0.23	0.95
FY16-2	Measured Vapor Pressure, Drying	0.607	0.000	8.48E-06	1.57	0.36	0.96
	Measured Vapor Pressure, Wetting	0.607	0.000	7.20E-06	1.55	0.35	0.94
	Measured Vapor Pressure, Combined	0.607	0.000	7.55E-06	1.59	0.37	0.94
	Controlled Vapor Pressure	0.607	0.000	1.57E-05	1.24	0.20	0.99
FY16-3	Measured Vapor Pressure, Drying	0.615	0.000	7.59E-06	1.54	0.35	0.96
	Measured Vapor Pressure, Wetting	0.615	0.000	9.10E-06	1.48	0.32	0.92
	Measured Vapor Pressure, Combined	0.615	0.000	8.30E-06	1.50	0.33	0.94
	Controlled Vapor Pressure	0.615	0.000	1.82E-05	1.24	0.19	0.97
FY16-4	Measured Vapor Pressure, Drying	0.601	0.000	6.42E-06	1.61	0.38	0.94
	Measured Vapor Pressure, Wetting	0.601	0.000	5.70E-06	1.63	0.39	0.86
	Measured Vapor Pressure, Combined	0.601	0.000	5.57E-06	1.63	0.39	0.91
	Controlled Vapor Pressure	0.601	0.000	7.94E-06	1.31	0.24	0.98

[1]Data analyzed using Mualem relationship between n and m where $m = 1 - 1/n$.
[2]θ_s fixed to average measured porosity for Secondary Waste analysis.

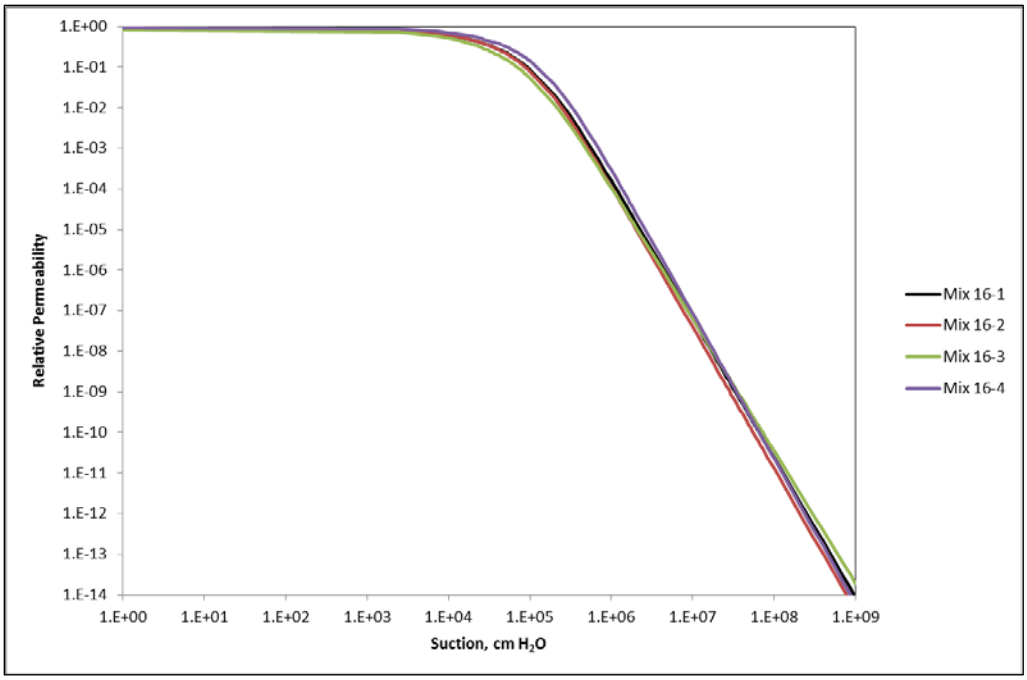

Figure 5-9. Comparison of relative permeability curves for Secondary Waste Mixes (Measured Vapor Pressure).

5.3 Quality Assurance

The work scope was performed in accordance with a Quality Assurance Program (QAP) that meets the Quality Assurance criteria specified in DOE Order 414.1D, Quality Assurance; 10 CFR 830, "Nuclear Safety Management," Subpart A, "Quality Assurance Requirements," paragraph 830.122; and also meets the requirements of ASME NQA-1-2004, Quality Assurance Requirements for Nuclear Facility Applications, including NQA-1a-2005 and NQA-1b-2007 Addenda, or later version. The work scope was performed in accordance with Savannah River Site Manual 1Q, QAP 2-3 (Control of Research and Development Activities). Requirements for performing reviews of technical reports and the extent of review are established in manual E7 2.60. SRNL documents the extent and type of review using the SRNL Technical Report Design Checklist.[49]

6.0 Conclusions

A Hanford Liquid Secondary Waste simulant was prepared representing the ETF evaporator concentrate (brine) in the DFLAW flowsheet. Five grout mixes were prepared with this simulant varying the water to dry materials blend and the dry materials blend composition.

As in previous testing, during mixing, the introduction of the dry blends into the waste simulant resulted in noticeable quantities of ammonia from the waste simulant being released. Based on results in Reference 1, this testing increased the W/DM to provide additional water for hydration of the grout mixes. Even with the additional water present, an admixture was required to modify rheological properties of the mixes. The gel times for the mixes ranged from >5 minutes to >120 minutes. Gel time measurements contain considerable variability. Gel times among replicates have been shown to vary up to 25%.[22] The structure developed in the mixes with gel times shorter than 20 minutes do not affect waste form properties, but can introduce operational challenges in a facility to recover from interruptions in processing. Mix FY16-5 did not set fully in 24 hours. Nor did it set in time for the 28 day compression test and was eliminated from further testing. Two formulations, mixes FY16-4 and FY16-5, contained free liquids after 24 hours. Mix FY16-5 had significant free water after 24 hours and retained free liquids

after 72 hours. The free liquid associated with Mix FY16-4 was reabsorbed into the waste form before the third day. Mix FY16-4 contained the most blast furnace slag. The neutral pH of the waste simulants do not accelerate the hydration of the blast furnace slag in the same way as caustic waste simulants.[50] The grout flowability was affected by the W/DM and the dry blend composition. An increase in W/DM led to an increase in grout flowability. Mix FY16-5 did not contain any hydrated lime, therefore the early reaction with the sulfate waste simulant to form ettringite was not present and resulted in extended grout flow. The yield stresses of the mixes tested were lower than the yield stresses measured in Reference 1. An increase in W/DM reduced the yield strength. A mix with a high yield stress will not affect cured properties, but may require additional consideration for routine waste treatment operations. The plastic viscosity of the mixes in this study were greater than for grouts tested in previous work.[1] It is likely that the increased sulfate in the simulant in this work provided for formation of additional ettringite solids, thus raising the plastic viscosity.

Results from the isothermal calorimetry testing, along with the heat rise measured during mixing—not measured in this task, but assumed present based on FY15 results— indicated that the reactions that occurred during mixing and the early stages of curing generated the majority of the heat created in these formulations. Because the waste simulants are near neutral, a portion of the heat generated may be attributed to the heat of reaction of the hydrated lime with the waste solution, rather than solely caused by heat of hydration. This may be caused by the test method not capturing the early heat generated during mixing and, insufficient water to complete hydration.

The compressive strength (28 day) of all of the mixes prepared with hydrated lime exceeded the target of 3.4 MPa (500 psi) to meet the requirements identified in Reference 3. The compressive strength was dependent on the W/DM ratio, with samples made using a W/DM of 0.60 having a greater compressive strength than samples prepared with a W/DM of 0.75. In addition to the 28-day cure, mix FY16-1 was tested after three and seven days. Sufficient strength was developed after seven days of curing to exceed the requirements in Reference 3. The mix made without hydrated lime did not develop sufficient structure to be tested.

The hydraulic conductivities of the mixes were measured using a flexible wall permeameter. The measured hydraulic conductivity was comparable to the results in Reference 1. The higher W/DM used in this work reduced or eliminated the consumption of permeant during the saturated hydraulic conductivity testing.

The relative permeability function produced using measured vapor equilibrium and controlled vapor are similar.

7.0 Recommendations

- Samples should be stored for greater than the current 28 day cure time prior to testing properties related to hydraulic properties. Ettringite, the primary phase formed in these formulations,[51] has not been tested over longer time frames like the calcium silicate hydrate based waste forms. If this waste form is to be considered for this waste stream, long term testing of hydraulic properties should be performed.
- Samples should be exposed to more realistic environmental conditions possible in the IDF.
- Prepare simulants based on ammonia destruction testing to evaluate alternative waste forms.[52]

8.0 References

[1] Cozzi, A.D., Dixon, K.L., Hill, K.A., King, W.D., and Nichols, R.L., Liquid Secondary Waste: Waste Form Formulation and Qualification, SRNL-2015-00685, Revision 1, Savannah River National Laboratory, Aiken, South Carolina, April 2016.

[2] D.L. Halgren, Effluent Treatment Facility Mass Balance Calculation for DFLAW Mission, HNF-58821, Revision 0, CH2MHill, P.O. Box 1600, Richland, Washington 99352, July 2015.

[3] Ramsey, A.A. Secondary Liquid Waste Treatment Cast Stone Technology Development Plan, RPP-51790, Revision 0, Washington River Protection Solutions, Richland, Washington, July 2012.

[4] Brown, E.E., Kelly, S. E., and Swanberg, D. J. Hanford Integrated Disposal Facility Performance Assessment Technology Support Program Plan, RPP-PLAN-60520, Revision 0, Washington River Protection Solutions, Richland, Washington, August 2015.

[5] Swanberg, D. R., Liquid Secondary Waste Formulation Development and Waste Form Qualification, Request for Proposal #282524, Revision 0, Washington River Protection Solutions, Richland, Washington, September, 2015.

[6] Cozzi, A. D., Task Technical and Quality Assurance Plan for the Liquid Secondary Waste Formulation Development and Waste Form Qualification, SRNL-RP-2016-00199 Revision 0, Savannah River National Laboratory, Aiken, South Carolina, April 2016.

[7] Cozzi. A. D., Fox, K. M., Hansen, E. K., and Roberts, K. A., Supplemental Immobilization of Hanford Low-Activity Waste: Cast Stone Augmented Formulation Matrix Tests, SRNL-STI-2014-00619, Revision 0, Savannah River National Laboratory, Aiken, South Carolina, July 2015.

[8] Um, W., Liquid Secondary Waste Grout Formulation Development and Testing, TP-SWCS-009, Revision 0.0, Pacific Northwest National Laboratory, Richland, Washington, February 2016.

[9] Inductively Coupled Plasma-Atomic Emission Spectrometer Agilent 730 ES, L29 ITS-0079.

[10] Anion Analysis Using the Dionex DX-500 and ICS-5000 Ion Chromatograph, L29 ITS-0027.

[11] Ion Chromatography System Operation for Sample Analysis, L16.12 AD-ISO-0013 Revision 1.

[12] Analysis of Ions in Solutions using a Dionex ICS3000 Ion Chromatography System, L16.1 ADS-2310.

[13] Weight Percent Solids Determination Using a Furnace or Oven, L29 ITS-0078, Revision 1.

[14] Operation of Mettler Toledo Hr73 Halogen Moisture Analyzer, L29 ITS-0007, Revision 2.

[15] Cozzi, A. D., Preparation and Characterization of a Simulant for the FY16 Liquid Secondary Waste Formulation Development and Waste Form Qualification Testing, SRNL-L3300-2016-00017, Revision 0, Savannah River National Laboratory, Aiken, South Carolina June, 2016.

[16] Standard Specification for Portland Cement, ASTM, West Conshohocken, PA, C 150/150M – 12.

[17] Standard Specification for Slag Cement for Use in Concrete and Mortars, ASTM, West Conshohocken, PA, C989/989M-14.

[18] Standard Specification for Coal Fly Ash and Raw or Calcined Natural Pozzolan for Use in Concrete, ASTM, West Conshohocken, PA, C618-12a

[19] Cooke, GA, LL Lockrem, M Avila, and RA Westberg. 2006. Effluent Treatment Facility Waste Stream Monolith Testing Phase II, RPP-RPT-31077, CH2M Hill Hanford Group, Richland, WA.

[20] Standard Specification for Chemical Admixtures for Concrete, ASTM, West Conshohocken, PA, C494/494M-13.

[21] Merlini, M., Artioli, G., Cerulli, T., Cella, F., and Bravo, A., Tricalcium Aluminate Hydration in Additivated Systems. A Crystallographic Study by SR-XRPD, Cement and Concrete Research, Vol. 38, pp. 477–486, 2008.

[22] Harbour, J.R., Edwards, T.B., Hansen, E.K., and Williams, V.J., Variability Study for Saltstone, WSRC-TR-2005-00447, Revision 0, Savannah River National Laboratory, Aiken, South Carolina, October 2005.

[23] Standard Test Method for Time of Setting of Hydraulic Cement by Vicat Needle, ASTM, West Conshohocken, PA, ASTM C 191-13.

[24] Monitoring Set Time of Grout Using Ultrasonic Pulse Velocity (UPV) System, ITS-WI-0044.
[25] Standard Test Method for Flow Consistency of Controlled Low Strength Material (CLSM), ASTM, West Conshohocken, PA, D 6103 – 04.
[26] Standard Practice for Measuring Hydration Kinetics of Hydraulic Cementitious Mixtures Using Isothermal Calorimetry, ASTM, West Conshohocken, PA, C 1679-09.
[27] Standard Test Method for Density of Liquid Coatings, Inks, and Related Products, ASTM, West Conshohocken, PA, D 1475-13.
[28] Hansen, E.K. and Langton, C.A., Physical Characterization of FY2004 Saltstone Simulant Studies, WSRC-TR-2005-00365 Savannah River National Laboratory, Aiken, South Carolina, December 2005.
[29] Haake RheoStress (RS) Rheometers, L29 ITS-0073.
[30] Cozzi, A.D., Fox, K.M., Hansen, E.K., and Roberts, K.A., Supplemental Immobilization of Hanford Low-Activity Waste: Cast Stone Augmented Formulation Matrix Tests, SRNL-STI-2014-00619 Revision 0, Savannah River National Laboratory, Aiken, South Carolina, 2015.
[31] Ferraris, C. F., Obla, K. H., and Hill, R., The Influence of Mineral Admixtures on the Rheology of Cement Paste and Concrete, Cement and Concrete Research, Volume 31, pp 245-255, 2001.
[32] Banfill, P. F. G., The Rheology of Fresh Cement and Concrete – A Review, Proc 11th Cement Chemistry Congress, May 2003.
[33] Palacios, M. and Puertas, F., Effect of Superplasticizer and Shrinkage-Reducing Admixtures on Alkali-Activated Slag Pastes and Mortars, Cement and Concrete Research, Vol. 35, pp. 1358– 1367, (2005).
[34] Fan, W., Stoffelbach, F., Rieger, J., Regnaud, L., Vichot, A., Bresson, B., and Lequeux, N., A New Class of Organosilane-Modified Polycarboxylate Superplasticizers with Low Sulfate Sensitivity, Cement and Concrete Research, Vol. 42, pp. 166–172, (2012).
[35] Standard Test Method for Compressive Strength of Cylindrical Concrete Specimens, ASTM, West Conshohocken, PA, C39/C39M – 15a.
[36] Standard Practice for Use of Unbonded Caps in Determination of Compressive Strength of Hardened Concrete Cylinders, ASTM, West Conshohocken, PA, C1231/C1231M – 14.
[37] Standard Test Method for Specific Gravity of Soil Solids by Gas Pycnometer, ASTM, West Conshohocken, PA, D5550-14.
[38] Harbour, J.R., Williams, V.J., Edwards, T.B., Eibling, R.E., Schumacher, R.F., Saltstone Variability Study – Measurement of Porosity, WSRC-STI-2007-00352 Revision 0, Savannah River National Laboratory, Aiken, South Carolina, 2007.
[39] Standard Test Methods for Measurement of Hydraulic Conductivity of Saturated Porous Materials Using a Flexible Wall Permeameter, ASTM, West Conshohocken, PA, D5084-10.
[40] Standard Test Methods for Determination of the Soil Water Characteristic Curve for Desorption Using Hanging Column, Pressure Extractor, Chilled Mirror Hygrometer, or Centrifuge, ASTM, West Conshohocken, PA, D 6836– 02 (Reapproved 2008).
[41] Harbour, J. R. , Williams, V. J. and Edwards, T. B., Heat of Hydration of Saltstone Mixes – Measurement by Isothermal Calorimetry, WSRC-STI-2007-00263 Revision 0, Savannah River National Laboratory, Aiken, South Carolina, 2007.
[42] Zhou, Q. and Glasser, F.P., Thermal stability and decomposition mechanisms of ettringite at <120 °C, Cement and Concrete Research, 31, 1333–1339. 2001.
[43] Van Genuchten, M. Th., A Closed-form Equation for Predicting the Hydraulic Conductivity of Unsaturated Soils, Soil Science Society of America Journal, v44, 892-898. 1980.
[44] Nimmo, J. R. and Winfield, K. A., Water Retention and Storage: Miscellaneous Methods. p 710-711. In J. H. Dane and G. C. Topp (ed.), Methods of Soil Analysis, Part 4, Physical Methods, Soil Science Society of America. 2002.

[45] Gee, G. W., Campbell, M. D., Campbell, G. S., and Campbell, J. H., Rapid Measurement of Low Soil Water Potentials using a Water Activity Meter. Soil Science Society of America Journal, v56, 1068-1070. 1992.

[46] Or, D., and Tuller, M., Liquid retention and interfacial area in variably saturated porous media: Upscaling from single-pore to sample-scale model, Water Resour. Res., 35(12), 3591-3606. 1999.

[47] Standard Practice for Maintaining Constant Relative Humidity by Means of Aqueous Solutions, ASTM, West Conshohocken, PA, E 104– 02 (Reapproved 2012).

[48] Brown, A. M., A Step-By-Step Guide To Non-Linear Regression Analysis Of Experimental Data Using A Microsoft Excel Spreadsheet. Computer Methods and Programs in Biomedicine, 65, 191-200. 2001.

[49] Butcher, B. T., Savannah River National Laboratory Technical Report Design Check Guidelines, WRSC-IM-2002-00011, Revision 2, Savannah River National Laboratory, Aiken, South Carolina, August 2004.

[50] Kim, M.S., Jun, Y., Lee, C., and Oh, J.E., Use of CaO as an Activator for Producing A Price-Competitive Non-Cement Structural Binder Using Ground Granulated Blast Furnace Slag, Cement and Concrete Research Volume 54, December 2013, Pages 208–214.

[51] Saslow, S.A., Um, W., Russell, R.L., Wang, G., Asmussen, R.M., and Sahajpal, R., Updated Liquid Secondary Waste Grout Formulation and Preliminary Waste Form Qualification, RPT-SWCS-009, Revision 0, Pacific Northwest National Laboratory, Richland, Washington, May 2017.

[52] Nash, C. A. and Fowley, M. D., Results of Initial Ammonia Oxidation Testing, SRNL-L3100-2016-00165, Revision 0, Savannah River National Laboratory, Aiken, South Carolina, 2017.

Appendix A Moisture Retention Data (Drying) Measured using a Chilled Mirror Humidity Sensor

Gravimetric Moisture Content (cm^3/cm^3)	Volumetric Moisture Content (cm^3/cm^3)	Saturation (fraction)	Total Potential (bar)	Total Potential (cm H_2O)
0.4888	0.500	0.84	98.7	100649
0.4179	0.428	0.72	134.5	137156
0.4093	0.419	0.70	163.4	166626
0.3958	0.405	0.68	164.8	168054
0.3461	0.354	0.59	279.6	285141
0.3443	0.352	0.59	244.0	248777
0.3375	0.345	0.58	266.3	271592
0.2901	0.297	0.50	444.7	453480
0.2889	0.296	0.49	420.4	428667
0.2750	0.281	0.47	564.8	575952
0.2508	0.257	0.43	699.3	713107
0.2413	0.247	0.41	689.7	703318
0.2269	0.232	0.39	952.9	981912
0.2195	0.225	0.38	1005.4	1035397
0.2058	0.211	0.35	981.7	1011229
0.1188	0.122	0.20	2931.8	3010081
0.1139	0.117	0.20	2745.8	2810211
0.1072	0.110	0.18	2801.2	2866705

Table A-1. Moisture Retention Data – Sample FY16-1, Drying.

Gravimetric Moisture Content (cm^3/cm^3)	Volumetric Moisture Content (cm^3/cm^3)	Saturation (fraction)	Total Potential (bar)	Total Potential (cm H_2O)
0.6326	0.611	1.02	64.6	65875
0.6251	0.603	1.01	61.1	62306
0.3761	0.363	0.61	172.0	175396
0.3734	0.360	0.60	185.1	188755
0.3356	0.324	0.54	232.7	237294
0.2992	0.289	0.48	318.4	324687
0.2991	0.289	0.48	358.2	365221
0.2735	0.264	0.44	437.8	446478
0.2441	0.236	0.39	678.0	691387
0.2394	0.231	0.39	615.4	627551
0.2265	0.219	0.37	772.7	787956
0.2055	0.198	0.33	837.7	854240
0.1988	0.192	0.32	839.7	856279
0.1976	0.191	0.32	798.1	813858
0.1834	0.177	0.30	1129.0	1151291
0.1730	0.167	0.28	1160.8	1183719
0.1656	0.160	0.27	1220.0	1254234
0.1089	0.105	0.18	2298.8	2344188
0.1024	0.099	0.17	2477.5	2526416
0.0888	0.086	0.14	2596.5	2657963

Table A-2. Moisture Retention Data – Sample FY16-2, Drying.

Gravimetric Moisture Content (cm^3/cm^3)	Volumetric Moisture Content (cm^3/cm^3)	Saturation (fraction)	Total Potential (bar)	Total Potential (cm H_2O)
0.6355	0.618	1.03	66.5	67813
0.4202	0.408	0.68	165.9	169176
0.3709	0.361	0.60	221.8	226179
0.3631	0.353	0.59	230.4	234949
0.3343	0.325	0.54	324.6	330958
0.3040	0.295	0.49	408.2	416260
0.3008	0.292	0.49	428.2	436655
0.2659	0.259	0.43	652.2	665077
0.2472	0.240	0.40	799.2	814980
0.2455	0.239	0.40	802.5	818311
0.2197	0.214	0.36	827.8	844144
0.2185	0.212	0.36	867.8	884934
0.2118	0.206	0.34	935.5	953971
0.1909	0.186	0.31	1295.7	1321232
0.1867	0.181	0.30	1291.6	1317102
0.1846	0.179	0.30	1307.1	1332857
0.1156	0.112	0.19	2518.9	2568634
0.1108	0.108	0.18	2496.0	2545282
0.1108	0.108	0.18	2417.8	2465538

Figure A-1. Moisture Retention Data – Sample FY16-3, Drying.

Gravimetric Moisture Content (cm^3/cm^3)	Volumetric Moisture Content (cm^3/cm^3)	Saturation (fraction)	Total Potential (bar)	Total Potential (cm H_2O)
0.6053	0.610	1.02	68.4	69751
0.6023	0.607	1.02	70.1	71484
0.5838	0.588	0.98	61.0	62204
0.3956	0.399	0.67	206.4	210475
0.3780	0.381	0.64	206.8	210883
0.3194	0.322	0.54	217.0	221285
0.3112	0.314	0.52	451.1	460007
0.2890	0.291	0.49	481.8	491313
0.2388	0.241	0.40	953.6	972428
0.2355	0.237	0.40	486.0	495545
0.2261	0.228	0.38	966.4	985481
0.1881	0.190	0.32	1264.4	1289365
0.1826	0.184	0.31	1091.5	1113051
0.1726	0.174	0.29	1750.2	1784756
0.1687	0.170	0.28	1095.5	1117130
0.1640	0.165	0.28	1573.9	1604925
0.1382	0.139	0.23	1162.9	1185861
0.1205	0.121	0.20	1581.7	1612930
0.1114	0.112	0.19	2590.0	2641138
0.0635	0.064	0.11	2377.6	2424544
0.0429	0.043	0.07	2294.8	2340109

Table A-3. Moisture Retention Data – Sample FY16-4, Drying.

Appendix B Moisture Retention Data (Wetting) Measured using a Chilled Mirror Humidity Sensor

Gravimetric Moisture Content (cm^3/cm^3)	Volumetric Moisture Content (cm^3/cm^3)	Saturation (fraction)	Total Potential (bar)	Total Potential (cm H_2O)
0.532	0.544	0.91	90.3	92082.9
0.477	0.481	0.80	107.9	110030.4
0.426	0.436	0.73	204.8	208843.6
0.356	0.359	0.60	367.9	375163.9
0.288	0.291	0.48	729.3	743699.5
0.267	0.273	0.46	411.7	419828.7
0.243	0.245	0.41	1043.1	1063695.3
0.234	0.239	0.40	621.5	633771.1
0.199	0.201	0.33	982.4	1001796.8
0.177	0.178	0.30	1325.2	1351365.1
0.158	0.162	0.27	828.6	844960.1
0.161	0.162	0.27	1690.5	1723877.7
0.147	0.151	0.25	1021.1	1041260.9
0.133	0.135	0.22	1589.8	1621189.5
0.130	0.131	0.22	1602.3	1633936.3

Table B-1. Moisture Retention Data – Sample FY16-1, Wetting.

Gravimetric Moisture Content (cm^3/cm^3)	Volumetric Moisture Content (cm^3/cm^3)	Saturation (fraction)	Total Potential (bar)	Total Potential (cm H_2O)
0.515	0.544	0.91	90.3	92082.91
0.458	0.481	0.80	107.9	110030.41
0.458	0.436	0.73	204.8	208843.63
0.377	0.359	0.60	367.9	375163.92
0.297	0.291	0.48	729.3	743699.51
0.277	0.273	0.46	411.7	419828.72
0.237	0.245	0.41	1043.1	1063695.27
0.248	0.239	0.40	621.5	633771.08
0.209	0.201	0.33	982.4	1001796.79
0.185	0.178	0.30	1325.2	1351365.13
0.178	0.162	0.27	828.6	844960.12
0.166	0.162	0.27	1690.5	1723877.72
0.165	0.151	0.25	1021.1	1041260.89
0.144	0.135	0.22	1589.8	1621189.47
0.136	0.131	0.22	1602.3	1633936.27

Table B-2. Moisture Retention Data – Sample FY16-2, Wetting.

Gravimetric Moisture Content (cm^3/cm^3)	Volumetric Moisture Content (cm^3/cm^3)	Saturation (fraction)	Total Potential (bar)	Total Potential (cm H_2O)
0.540	0.525	0.854	98.1	100036.9
0.477	0.481	0.799	122.5	124918.7
0.483	0.470	0.765	146.4	149290.6
0.390	0.393	0.654	271.7	277064.5
0.299	0.301	0.501	678.5	691896.5
0.315	0.306	0.498	301.6	307554.9
0.236	0.279	0.454	451.6	460516.5
0.287	0.238	0.395	1170.1	1193203
0.234	0.236	0.392	949.2	967941.3
0.205	0.207	0.343	1355.5	1382263
0.181	0.184	0.306	1800.4	1835948
0.182	0.176	0.287	778.4	793769
0.172	0.167	0.272	943.2	961822.8
0.150	0.151	0.252	1622.5	1654535
0.144	0.145	0.242	1667.7	1700628

Table B-3. Moisture Retention Data – Sample FY16-3, Wetting.

Gravimetric Moisture Content (cm^3/cm^3)	Volumetric Moisture Content (cm^3/cm^3)	Saturation (fraction)	Total Potential (bar)	Total Potential (cm H_2O)
0.519	0.523	0.870	117.5	119820
0.466	0.470	0.781	102.7	104727.7
0.458	0.462	0.768	236.1	240761.6
0.354	0.356	0.593	524.5	534855.9
0.297	0.300	0.499	834.6	851078.6
0.253	0.262	0.435	1015.3	1035346
0.125	0.255	0.424	373.2	380568.6
0.206	0.207	0.345	683.1	696587.3
0.148	0.160	0.266	792.6	808249.3
0.134	0.149	0.248	1334.4	1360747
0.159	0.140	0.233	1193.5	1217065
0.466	0.135	0.224	1678.5	1711641
0.139	0.126	0.210	1600.9	1632509
0.110	0.111	0.185	1954	1992580

Table B-4. Moisture Retention Data – Sample FY16-4, Wetting.

Appendix C Plots of the van Genuchten Curve Fit for each Formulation and Dataset

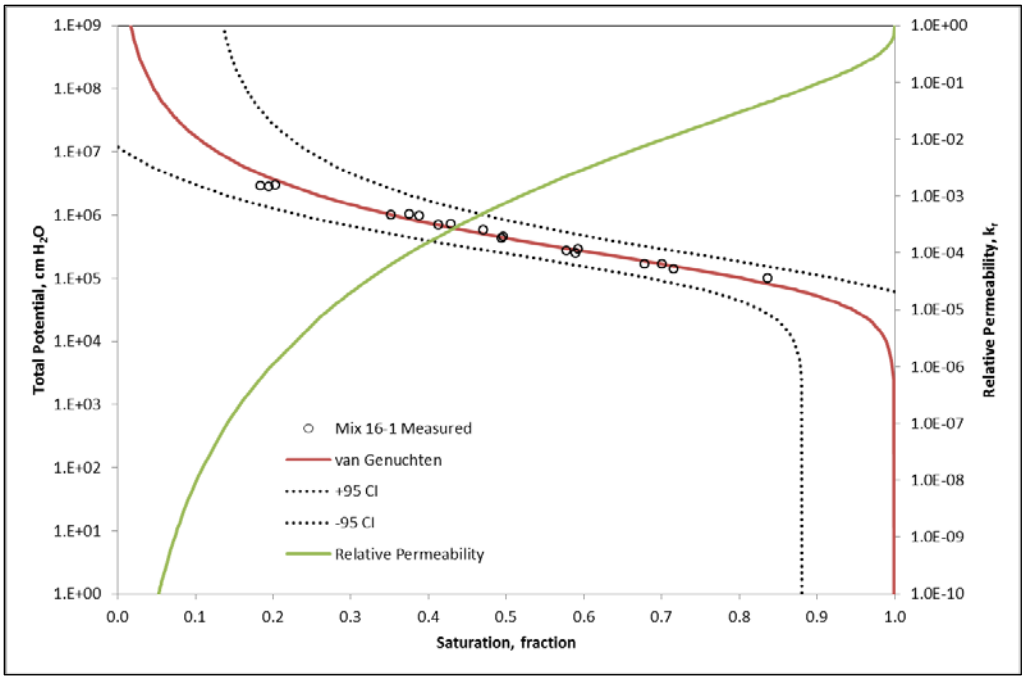

Figure C-1. Characteristic curves for Secondary Waste Mix 16-1 – Measured Vapor Pressure (Drying).

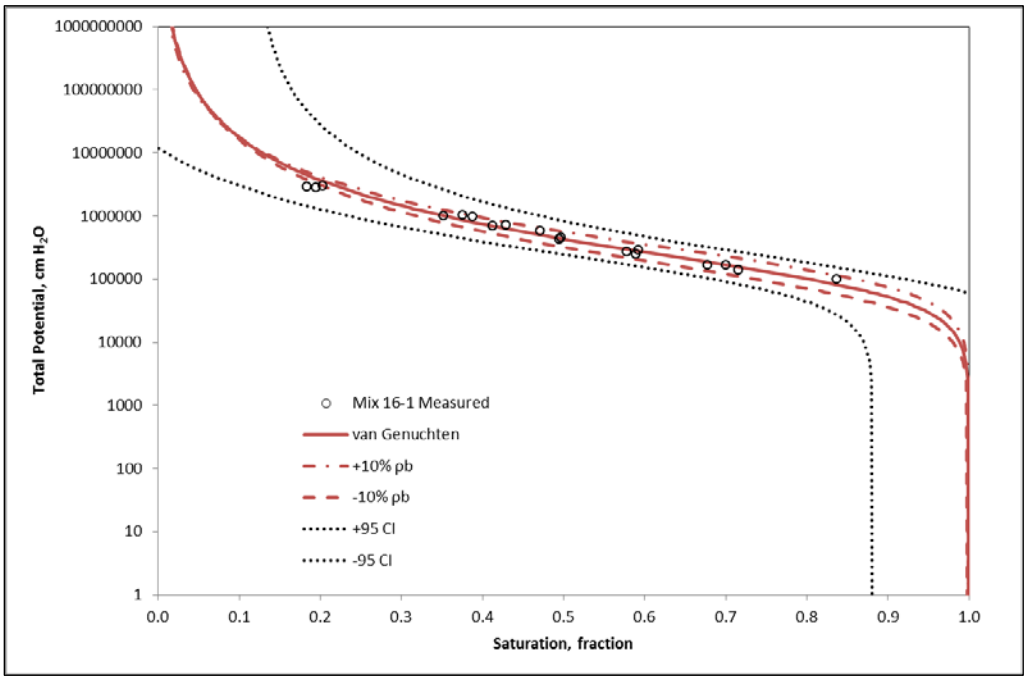

Figure C-2. Characteristic curves for Secondary Waste Mix 16-1 showing effect of ±10% dry bulk density.

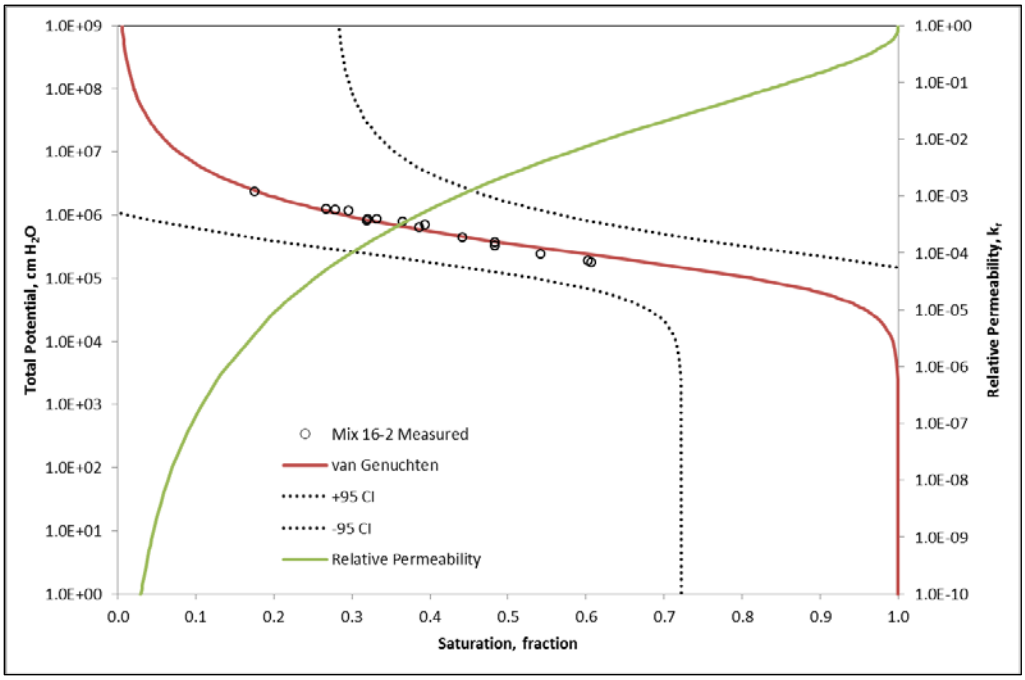

Figure C-3. Characteristic curves for Secondary Waste Mix 16-2 – Measured Vapor Pressure (Drying).

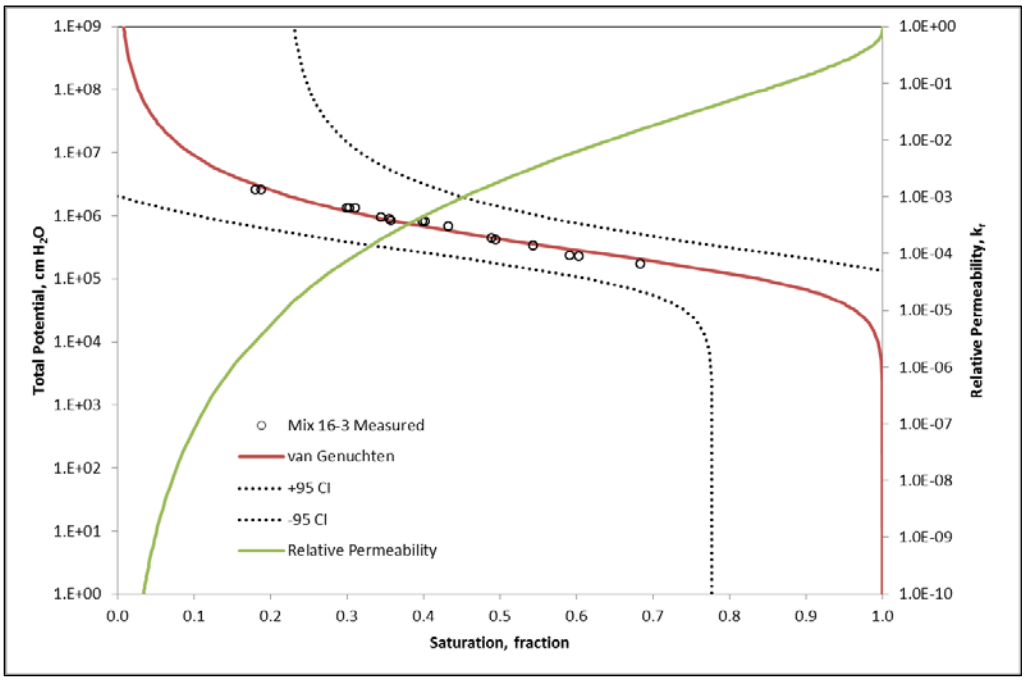

Figure C-4. Characteristic curves for Secondary Waste Mix 16-3 – Measured Vapor Pressure (Drying).

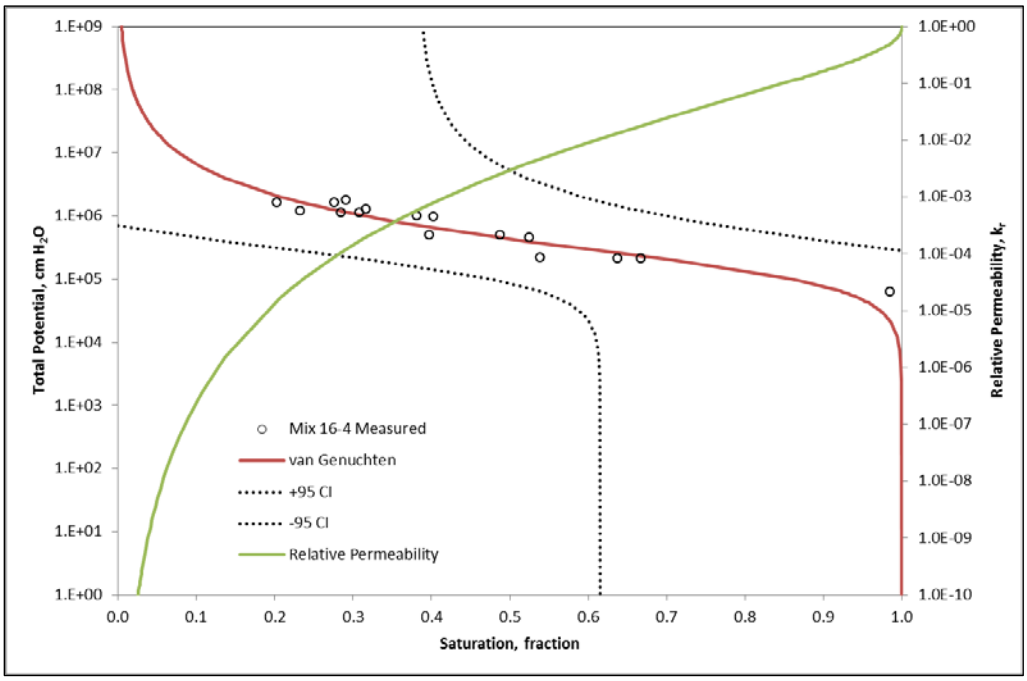

Figure C-5. Characteristic curves for Secondary Waste Mix 16-4 – Measured Vapor Pressure (Drying).

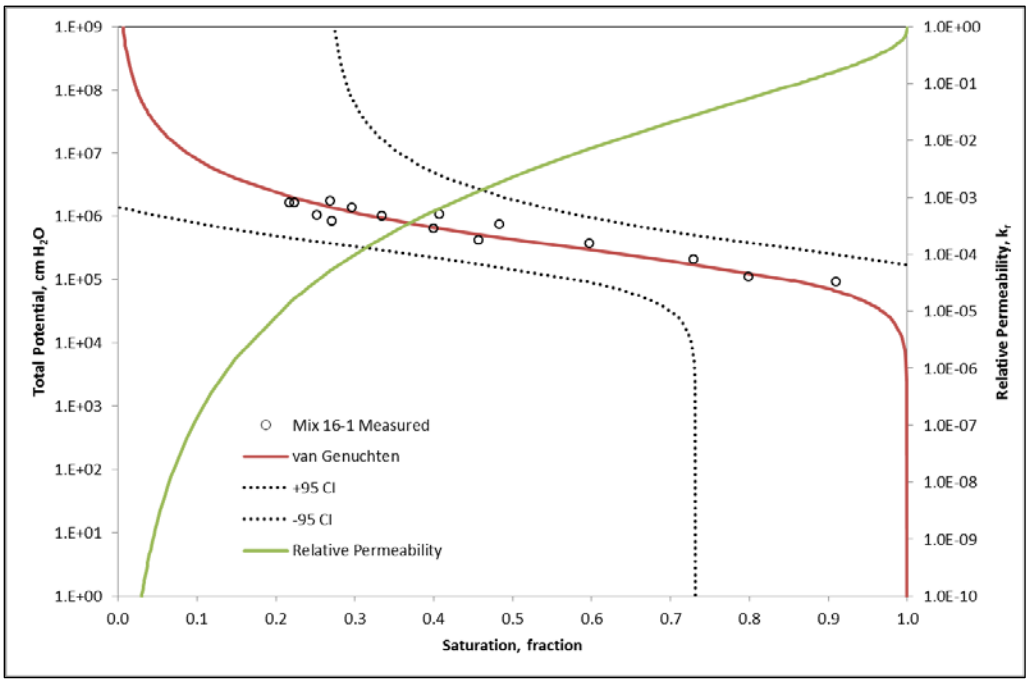

Figure C-6. Characteristic curves for Secondary Waste Mix 16-1 – Measured Vapor Pressure (Wetting).

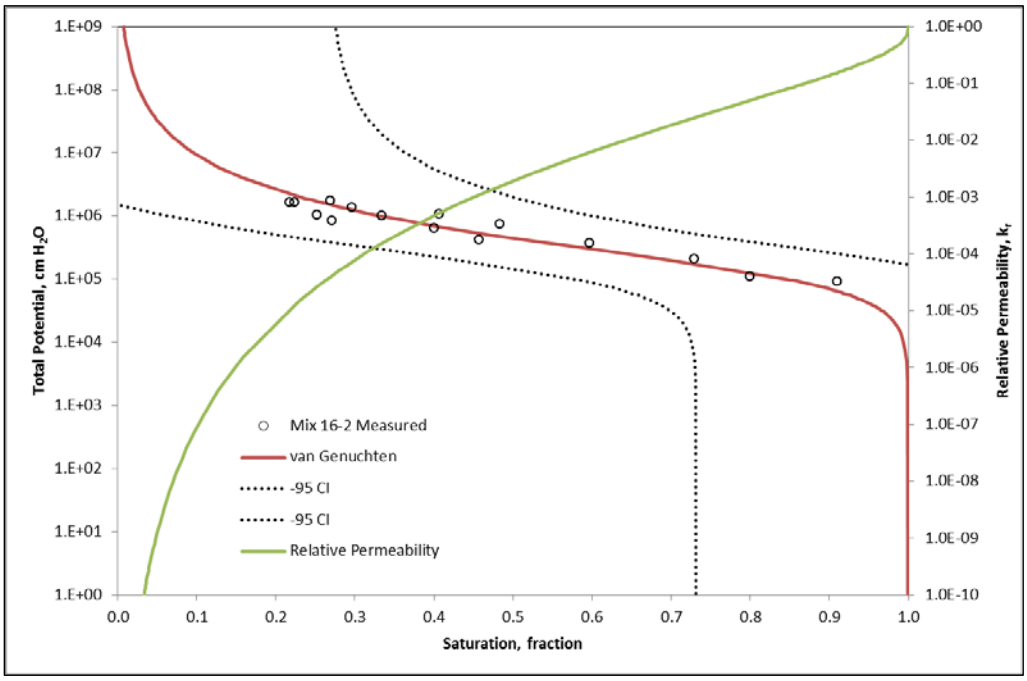

Figure C-7. Characteristic curves for Secondary Waste Mix 16-2 – Measured Vapor Pressure (Wetting).

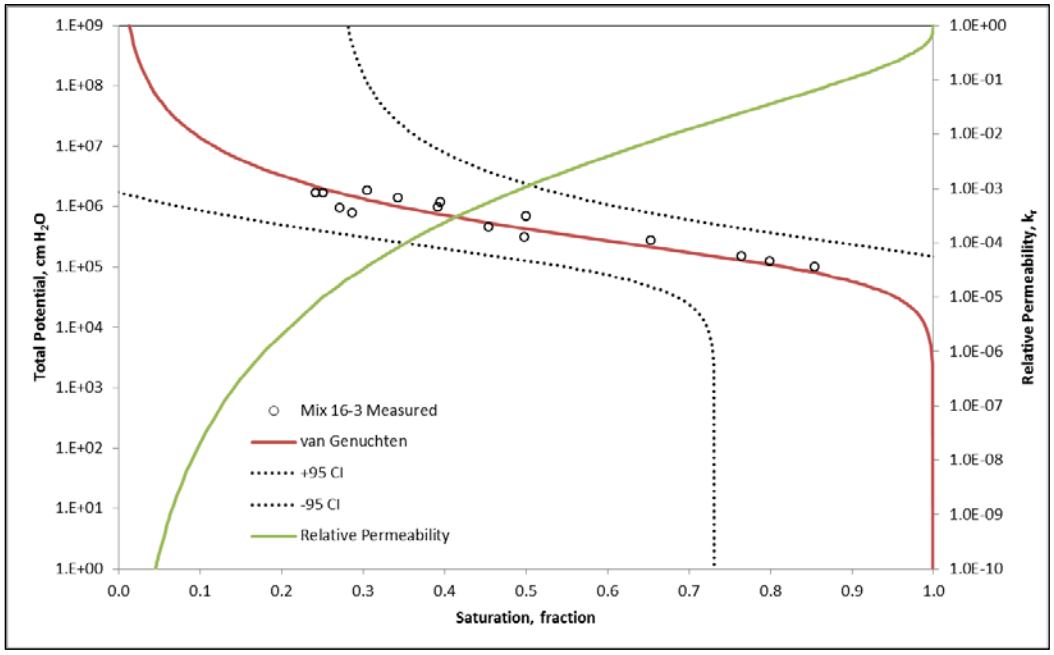

Figure C-8. Characteristic curves for Secondary Waste Mix 16-3 – Measured Vapor Pressure (Wetting).

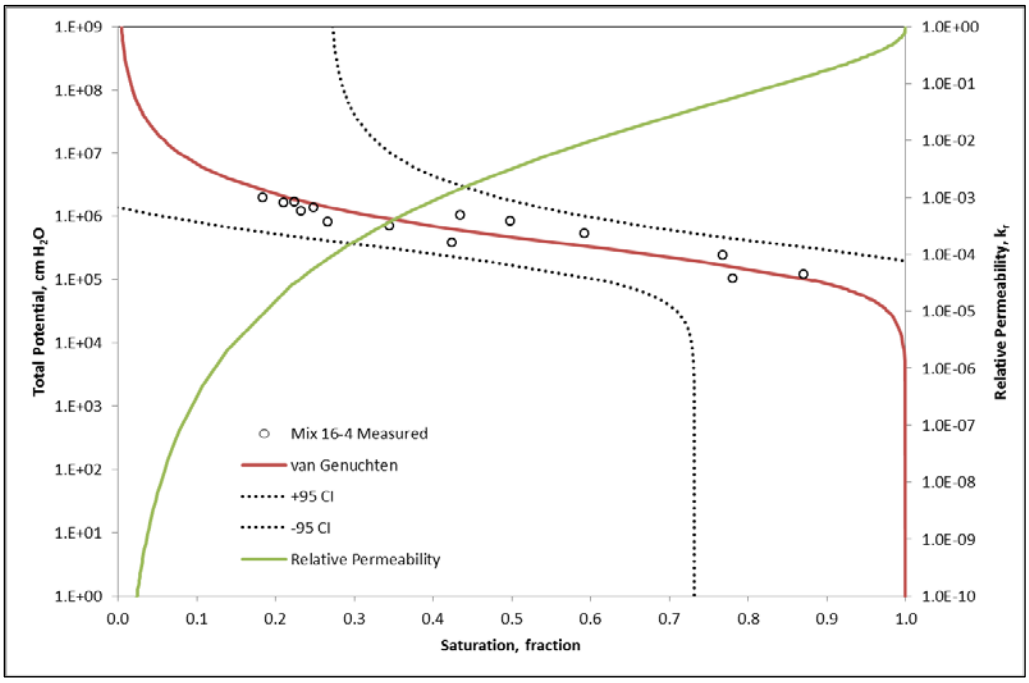

Figure C-9. Characteristic curves for Secondary Waste Mix 16-4 – Measured Vapor Pressure (Wetting).

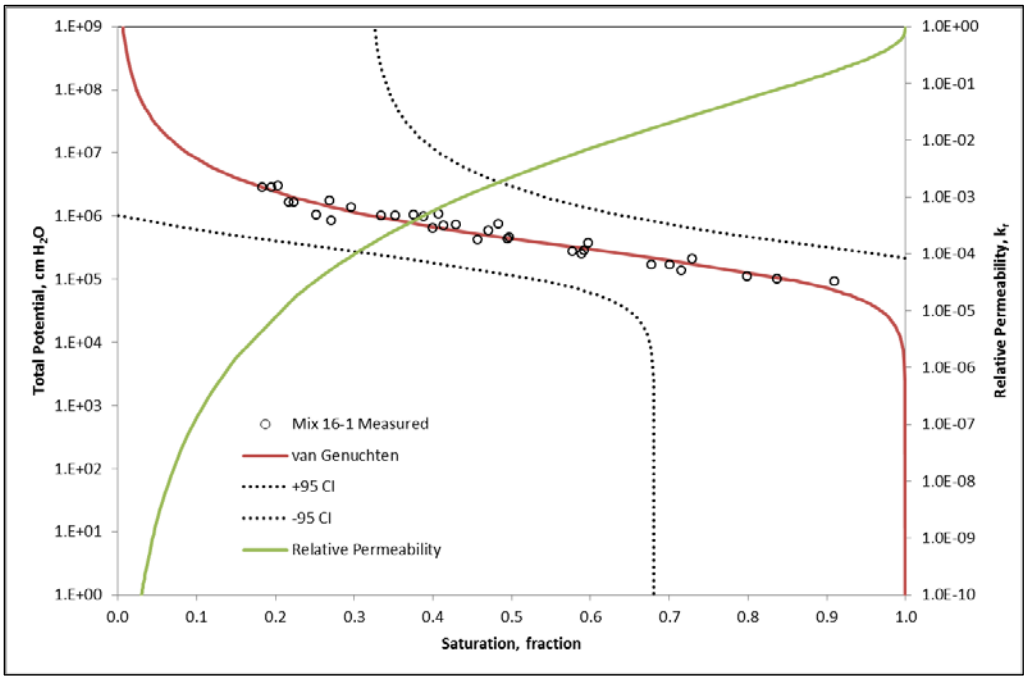

Figure C-10. Characteristic curves for Secondary Waste Mix 16-1 – Measured Vapor Pressure (Drying and Wetting Combined).

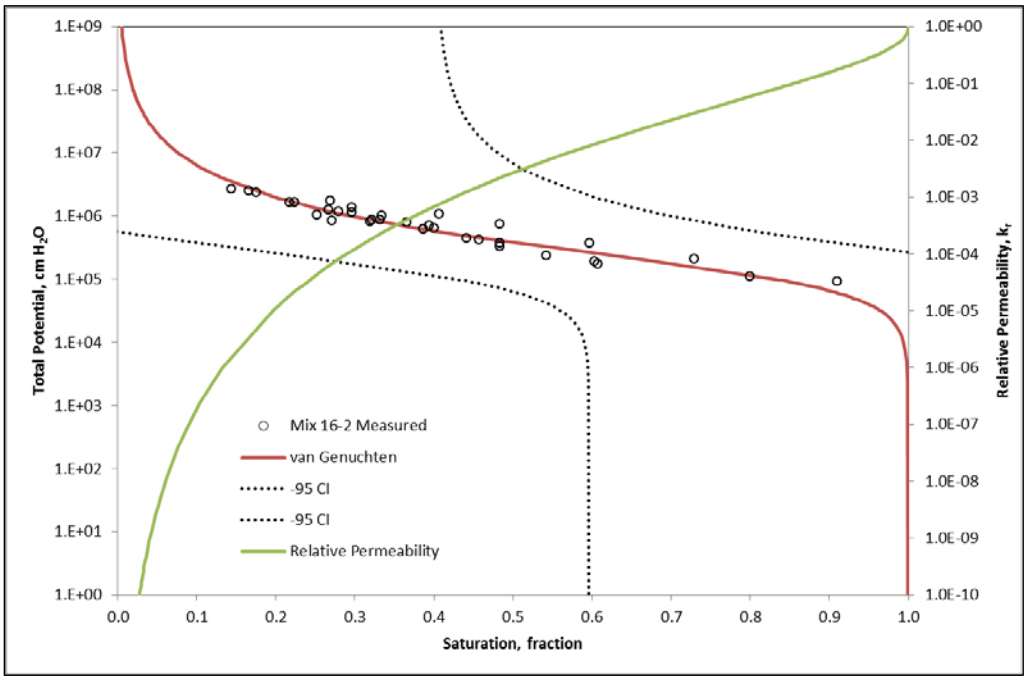

Figure C-11. Characteristic curves for Secondary Waste Mix 16-2 – Measured Vapor Pressure (Drying and Wetting Combined).

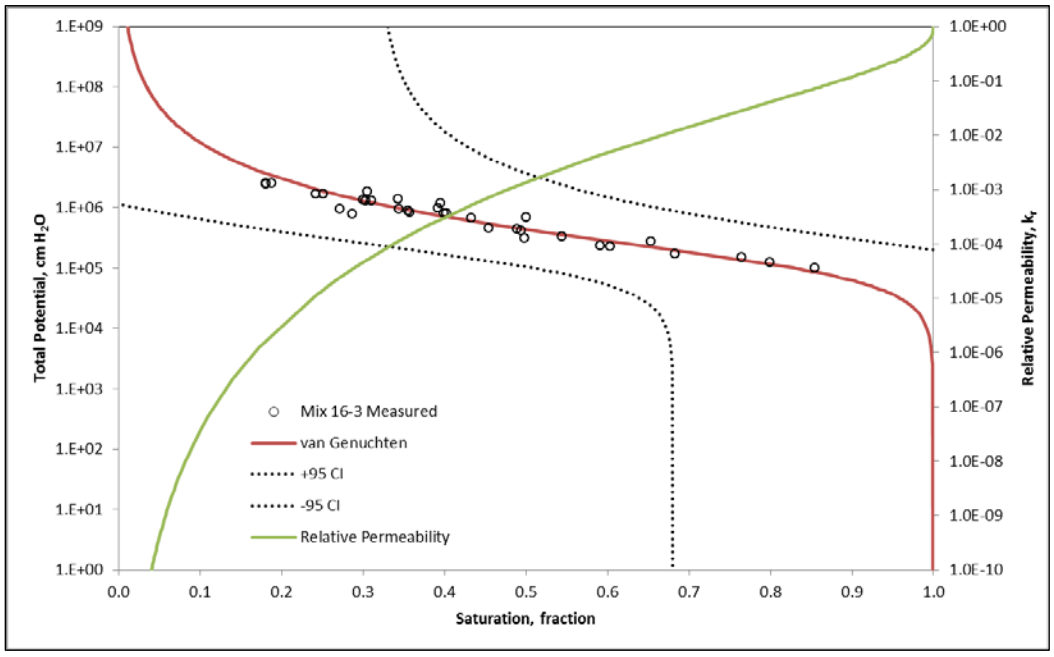

Figure C-12. Characteristic curves for Secondary Waste Mix 16-3 – Measured Vapor Pressure (Drying and Wetting Combined).

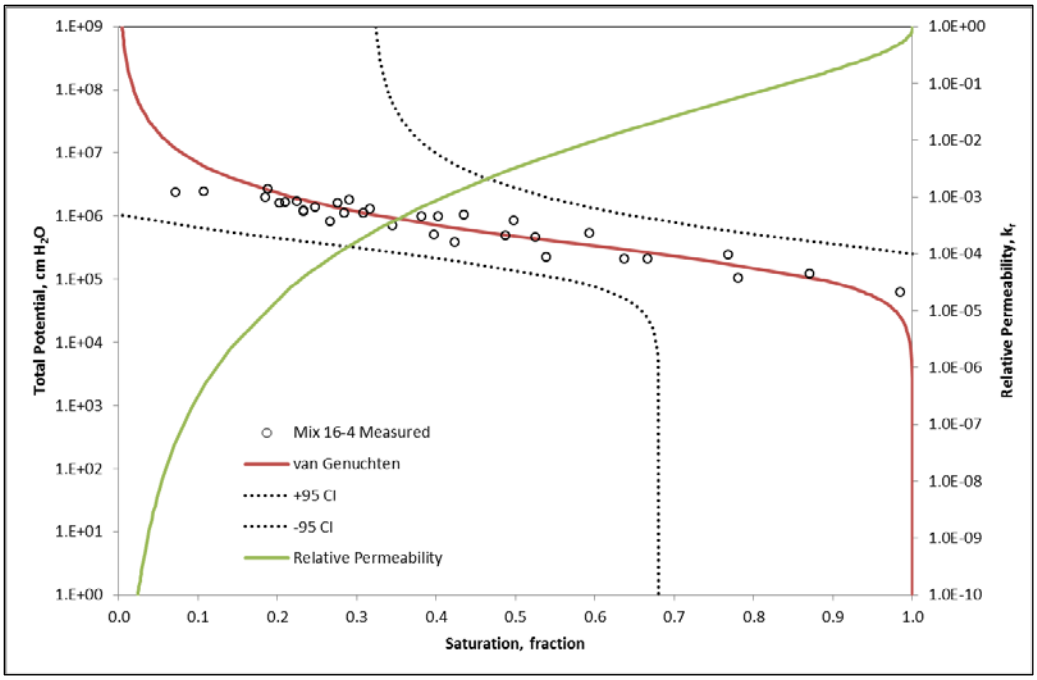

Figure C-13. Characteristic curves for Secondary Waste Mix 16-4 – Measured Vapor Pressure (Drying and Wetting Combined).

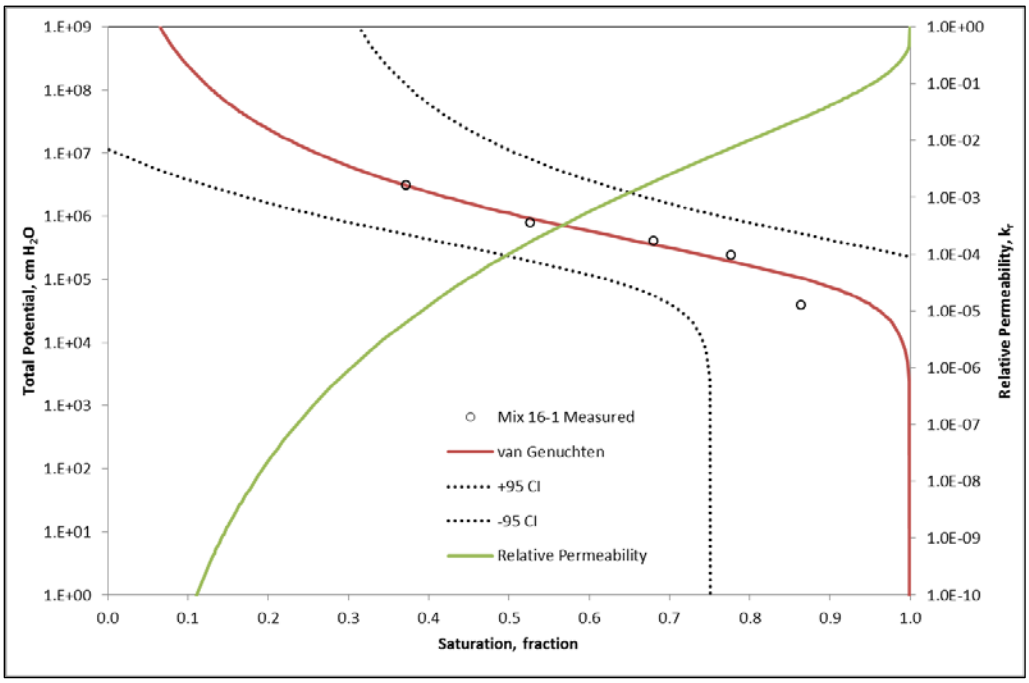

Figure C-14. Characteristic curves for Secondary Waste Mix 16-1 – Controlled Vapor Pressure.

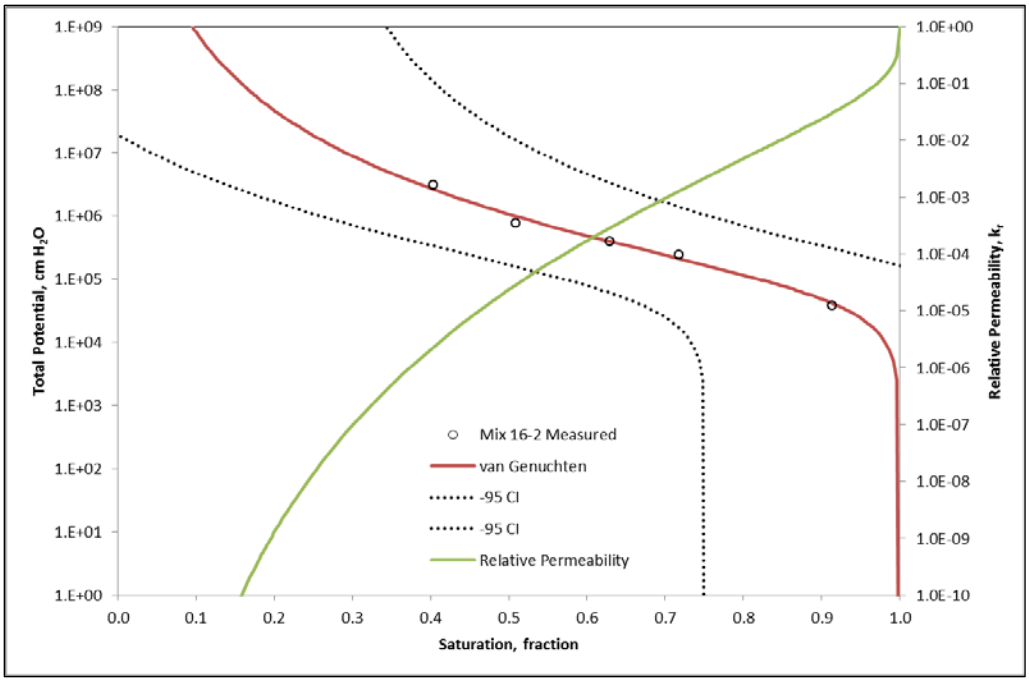

Figure C-15. Characteristic curves for Secondary Waste Mix 16-2 – Controlled Vapor Pressure.

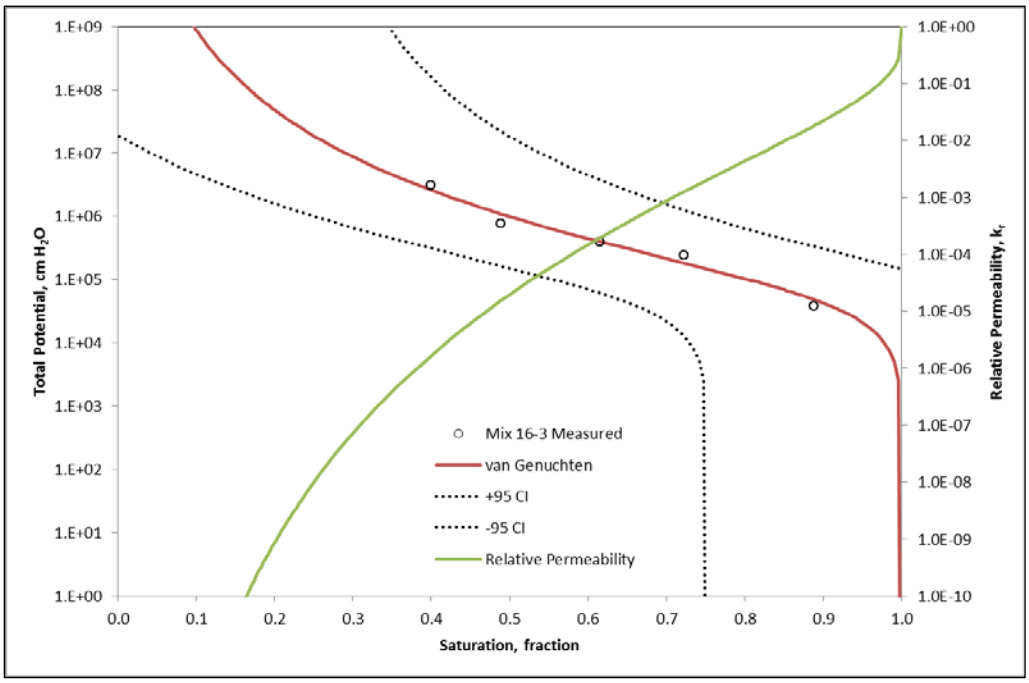

Figure C-16. Characteristic curves for Secondary Waste Mix 16-3 – Controlled Vapor Pressure.

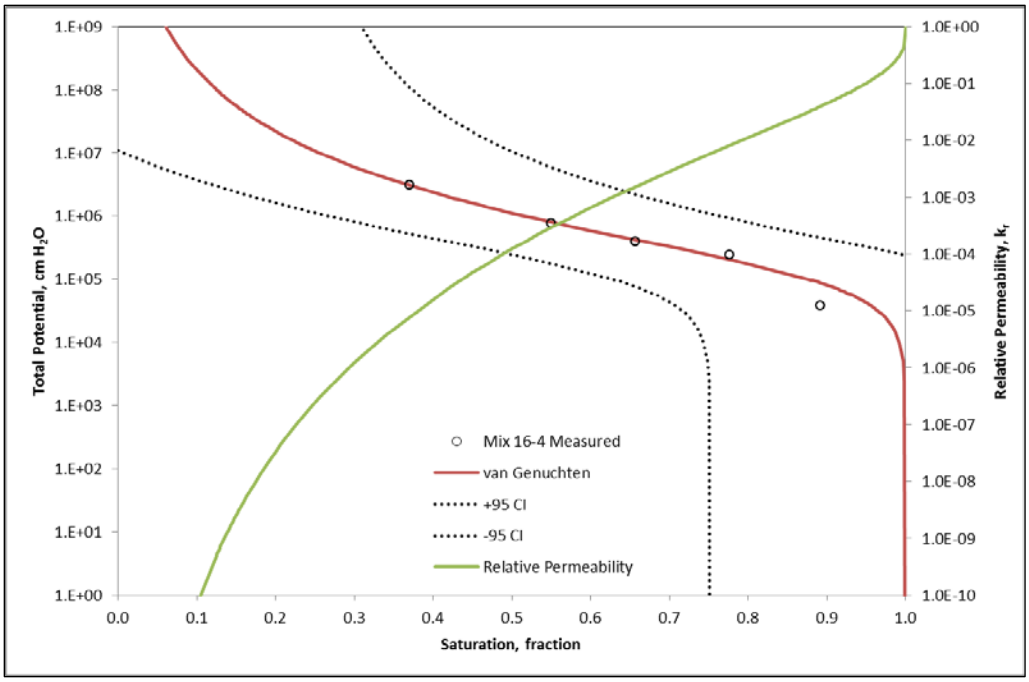

Figure C-17. Characteristic curves for Secondary Waste Mix 16-4 – Controlled Vapor Pressure.

.

Appendix D Plots of the Relative Permeability Function using the Combined Measured Vapor Equilibrium Dataset (Drying and Wetting).

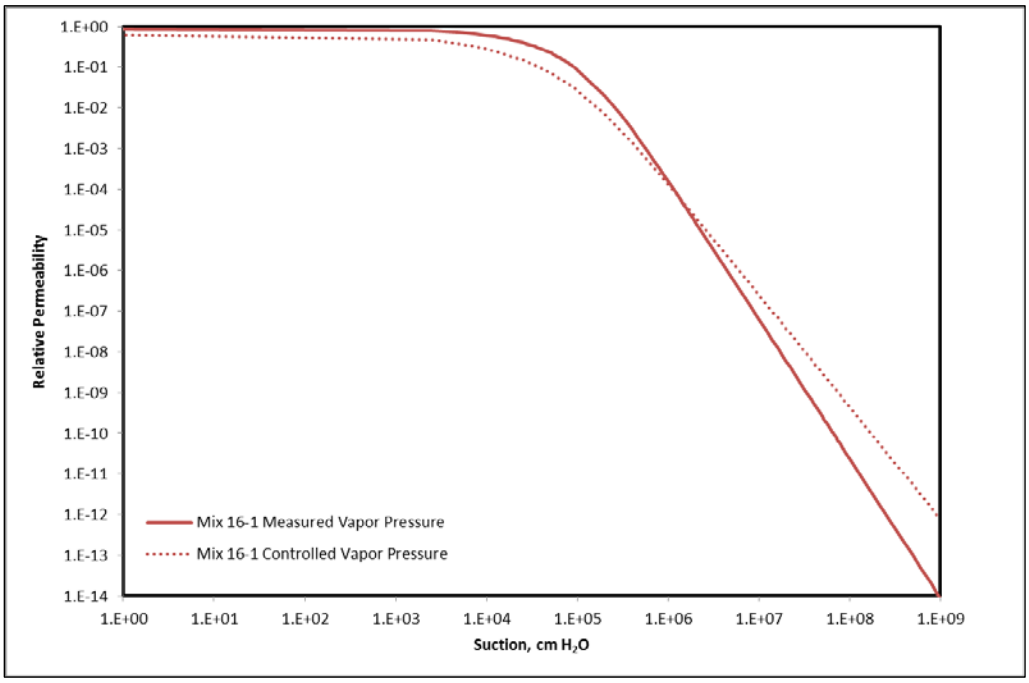

Figure D-1. Comparison of relative permeability curves for Secondary Waste Mix 16-1 using Measured and Controlled Vapor Pressure.

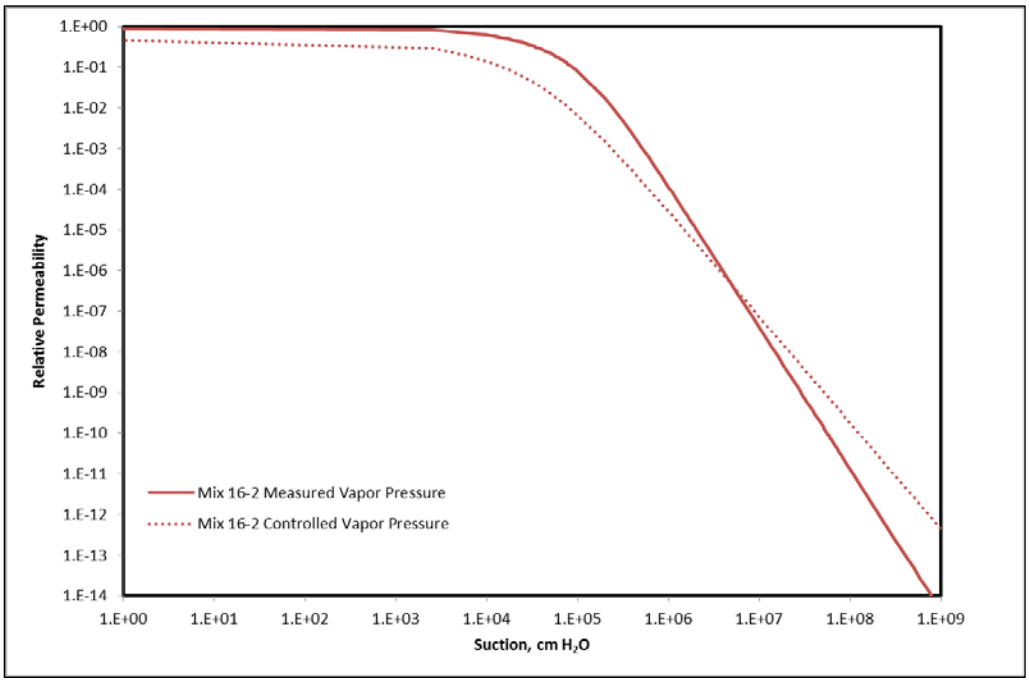

Figure D-2. Comparison of relative permeability curves for Secondary Waste Mix 16-2 using Measured and Controlled Vapor Pressure.

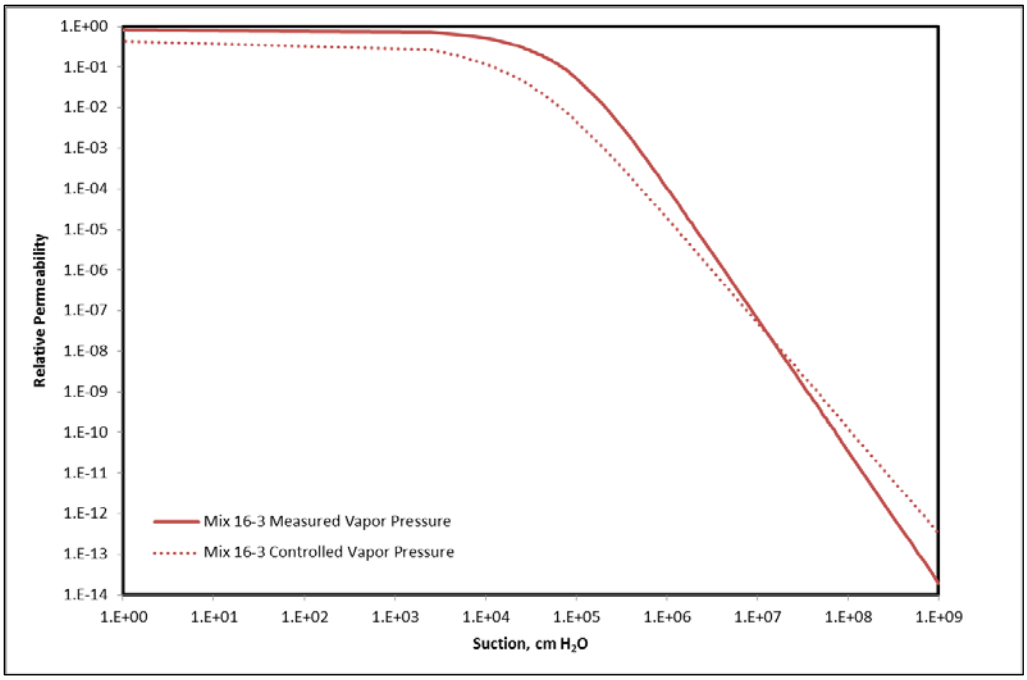

Figure D-3. Comparison of relative permeability curves for Secondary Waste Mix 16-3 using Measured and Controlled Vapor Pressure.

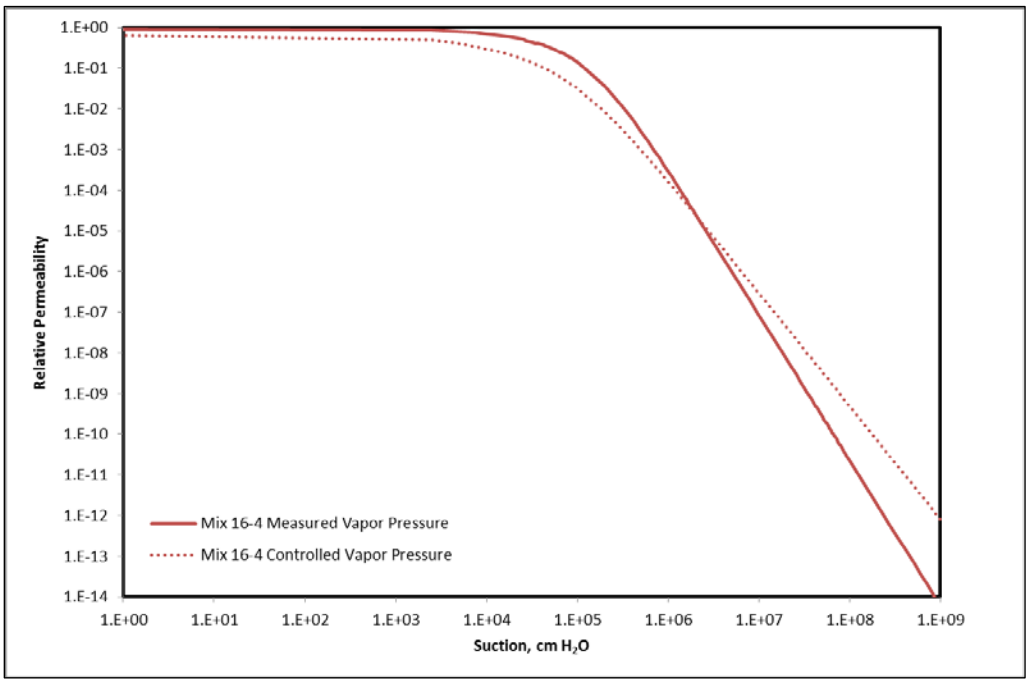

Figure D-4. Comparison of relative permeability curves for Secondary Waste Mix 16-4 using Measured and Controlled Vapor Pressure.

Distribution:

D. E.	Dooley,	773-A	D. T.	Herman,	735-11A
C. C.	Herman,	773-A	K. A.	Hill,	999-W
T. B.	Brown,	773-A	A. M.	Howe,	999-W
A. D.	Cozzi,	999-W	W. P.	Kubilius,	999-W
A. P.	Fellinger,	773-42A	C. M.	Jantzen,	773-A
G. A.	Morgan,	999-W	C.A.	Langton,	773-42A
E. N.	Hoffman,	999-W	M. H.	Lee,	
F. M.	Pennebaker,	773-42A	D. J.	McCabe	773-42A
B. J.	Weidenman	773-42A	D. L.	McClane,	999-W
J. W.	Amoroso,	999-W	F. R.	Miera	
H. H.	Burns,	773-41A	M. R.	Poirier,	773-42A
T. B.	Edwards,	999-W	A. A.	Ramsey,	999-W
S. D.	Fink,	773-A	W. G.	Ramsey,	999-W
M. D.	Fowley,	786-A	M. M.	Reigel,	773-42A
K. M.	Fox,	999-W	M. E.	Stone,	999-W
G. R.	Golcar		C. L.	Trivelpiece,	999-W
E. K.	Hansen,	999-W	W. R.	Wilmarth,	773-A

Records Administration (EDWS)

R. B. Mabrouki, WRPS (Ridha_B_Mabrouki@rl.gov)
D. J. Swanberg, WRPS (David_J_Swanberg@rl.gov)
J. R. Vitali, WRPS (Jason_R_Vitali@rl.gov)
R. H. Davis, WRPS (Renee_H_Davis@rl.gov)
S. T. Arm, WRPS (Stuart_T_Arm@rl.gov)
E. E. Brown, WRPS (Elvie_Brown@rl.gov)
G. Cooke, WRPS (Gary_Cooke@rl.gov)
T.A. Wooley, WRPS (Theodore_A_Wooley@rl.gov)

E. N. Diaz. DOE-ORP (elaine_n_diaz@orp.doe.gov)
N.M. Jaschke, DOE-ORP (naomi.jaschke@rl.gov)
B. M. Mauss, DOE-ORP (billie_m_mauss@orp.doe.gov)
R. A. Gilbert, DOE-ORP (robert_a_rob_gilbert@orp.doe.gov)
K. W. Burnett, DOE-ORP (kaylin.burnett@orp.doe.gov)
L. T. Nirider, DOE-ORP (laurren_t_nirider@orp.doe.gov)
G.L. Pyles, DOE-ORP (gary.pyles@orp.doe.gov)
W. R. Wrzesinski, DOE-ORP (wendell_r_wrzesinski@rl.gov)